

Geological features of the northeastern Canadian Arctic margin (Canada) revealed from analysis of potential field data

Goodluck K. Anudu^{1*}, Randell A. Stephenson¹, David I. M. Macdonald¹ and Gordon N. Oakey²

¹Department of Geology and Petroleum Geology, School of Geosciences, University of Aberdeen, Meston Building, King's College, AB24 3UE, Aberdeen, Scotland, UK.

²Geological Survey of Canada, Atlantic, 1 Challenger Drive, PO Box 1006, Dartmouth, Nova Scotia, B2Y 4A2, Canada.

*Corresponding author.

E-mail addresses: goodluck.anudu@abdn.ac.uk; anudugoodluck@yahoo.co.uk (G. K. Anudu), r.stephenson@abdn.ac.uk (R. A. Stephenson), d.macdonald@abdn.ac.uk (D. I. M. Macdonald), goakey@nrcan.gc.ca (G. N. Oakey).

Abstract

The northeastern Canadian Arctic margin is bordered to the north by Alpha Ridge, a dominantly magmatic complex within the Amerasia Basin of the Arctic Ocean, which forms part of the High Arctic Large Igneous Province (HALIP). The characteristics of the gravity and magnetic anomaly fields change notably along the Arctic margin, with two main segments recognised. Aeromagnetic and gravity data in the transition zone between these contrasting domains of the Canadian Arctic margin are analysed here in detail. Results obtained using a variety of edge enhancement (derivative) methods highlight several magnetic domains and a major offshore sedimentary basin as well as some known and a number of previously unknown tectonic and magmatic elements. A magmatic intrusion distribution map derived from the edge enhanced magnetic anomaly maps reveals that magmatic rocks are much more widespread in the relatively shallow subsurface than implied by surface geological mapping. Magmatic intrusions (mainly dykes) and other geological structures have NW-SE, NE-SW and N-S major trends. Broad gravity and pseudogravity lows across most of the Sverdrup Basin region are due to thick, less dense sedimentary succession and low magnetised crust. Magnetic and pseudogravity highs observed over Alpha Ridge indicate high crustal magnetisation associated with the occurrence of extensive and voluminous crustal magmatic bodies. Absence of these volcanic and intrusive rocks in the imaged sedimentary basin beneath the northeast Canadian Arctic margin region suggests that the basin probably formed after the cessation of HALIP magmatism.

Keywords: Canadian Arctic margin, gravity/magnetic data, magnetic domains, magmatic intrusions, pseudogravity, Alpha Ridge.

1. Introduction

The present northeast Canadian Arctic margin (CAM) encompasses the southern part of the offshore Alpha Ridge magmatic complex, Canadian Arctic Shelf and the central region of onshore Sverdrup Basin of the Canadian Arctic Islands (Figure 1). The subsurface geology and tectonic features of the onshore Sverdrup Basin are important for understanding the evolution of the Canadian Arctic margin. It has a complex geological and tectonic history and has been affected by extensive magmatic activity that resulted in the widespread emplacement of volcanic and intrusive rocks in the Early Cretaceous to Palaeogene.

[Insert Figure 1 about here]

Previous onshore geological (e.g. Trettin and Parrish, 1987; Embry and Osadetz, 1988; Okulitch, 1991; Trettin, 1991; Embry and Beauchamp, 2008; Harrison et al., 2011; Williamson et al., 2011) and potential field (e.g. Stephenson and Ricketts, 1990; Oakey and Stephenson, 2008; Oakey et al., 2012) studies conducted across the central region of the Late Palaeozoic to Palaeogene Sverdrup Basin have reported the presence of numerous flood basalts, thin lava flows, pyroclastics/tuffs, mafic dykes and sills of Cretaceous to Palaeogene age, including the Hansen Point Volcanics (HPV). Additionally, results from the few available seismic refraction experiments in the area (Asudeh et al., 1989; Argyle and Forsyth, 1994; Forsyth et al., 1998; Funck et al., 2011) have recognised the presence of notable sedimentary sub-basins on the offshore Canadian Arctic Shelf area. However, the detailed distribution and areal extent of these volcanic and intrusive igneous rock bodies emplaced on and within the underlying thick Mesozoic sedimentary successions across the Sverdrup Basin region, as well as the actual dimensions and relative time of development of the offshore marginal sedimentary sub-basins are not well known.

The purpose of this paper is to elucidate the regional subsurface geology and tectonics of the northeast CAM using potential field (gravity and magnetic) data, constrained with available geophysical and surface geological information. Specific objectives include mapping the detailed distribution of volcanic and intrusive igneous rock bodies, delineating the size/geometry of marginal offshore sedimentary sub-basins and making inferences on the relative timing of some major tectonic events affecting the northeast CAM.

2. Regional setting and character of potential field anomalies of the Canadian Arctic Margin

The Canadian Arctic Margin (CAM) extends for more than 2300 km from the northeastern tip of Ellesmere Island southwestwards to the Alaska border in the Beaufort Sea (Figure 1). It is generally believed to have developed as a rifted passive margin during the Mesozoic. Its age is widely considered to be Jurassic to Mid-Early Cretaceous, with its origin ascribed to a general counter-clockwise rotational opening of Canada Basin (the presumed oceanic part of the Amerasia Basin of the Arctic Ocean; cf. Chian et al., this volume) as Arctic Alaska and Chukchi/Northwind Ridge moved away from the Canadian Arctic Islands (e.g. Tailleux, 1973; Embry, 1990; Embry and Dixon, 1990; Moore et al., 1994; Grantz et al., 2011; Døssing et al. 2013a). This rotational model is supported by the presence of a curvilinear negative Free-Air gravity anomaly (i.e. gravity low designated as CBR on Figure 2) within Canada Basin inferred to be an extinct seafloor spreading ridge (e.g. Laxon and McAdoo, 1994; Grantz et al., 2011). Some authors have also cited various similarities in geology and geophysical character of the Canadian Arctic Islands, Arctic Alaska, Northwind Ridge and Chukchi Plateau (e.g. Embry, 1990; Embry and Dixon, 1990; Grantz et al., 2011; Gottlieb et al., 2014) although this remains a matter of considerable debate (e.g. Lane et al., 2016.) In any case, the CAM is generally considered to be a rifted, passive continental margin, the conjugate margin of which may at least in part be the Arctic Alaska Margin to the west with the Lomonosov Ridge margin to the north as a transform margin (e.g. Tailleux, 1973; Embry, 1990; Grantz et al., 2011). Most of subsurface geological bodies/features at the northeast CAM have been modified by extensive magmatic activities associated with the emplacement of Alpha Ridge igneous province in the Early Cretaceous, together with other younger magmatic and tectonic events such as the Eurekan Orogeny (Eocene – Oligocene).

The characteristics of the gravity and magnetic fields change notably along the CAM (Figure 2). Two major segments are recognised. First, the Beaufort Sea northeast to (approximately offshore) Axel Heiberg Island segment is characterised by large (50 – 180 km wide) NE-SW trending, semi-continuous positive elliptical gravity anomalies (gravity anomaly highs) with amplitudes in excess of 52 mGal and broad (40 – 110 km wide), negative (moderately low) magnetic anomalies. These elliptical gravity anomaly highs and moderately low magnetic anomalies (suppressed magnetic field) (Figure 2) tend to coincide with the 445 – 1900 m bathymetric depth contours (Figure 1) and are roughly restricted within the shelf-slope regions. The aforementioned gravity anomaly highs were named the Arctic margin gravity

highs by [Vogt et al. \(1998\)](#), whereas the corresponding negative magnetic anomalies are called the Polar Shelf Magnetic Anomaly (PSMA) by [Forsyth et al. \(1990\)](#).

[Insert Figure 2 about here]

Earthquake epicentre clusters locally coincide with regions of elliptical gravity anomaly highs and moderately magnetic anomaly lows along this segment of the CAM, especially those in the southern Beaufort Sea area and offshore northwest Ellef Ringnes Island (e.g. [Forsyth et al., 1990](#)). The first was interpreted by [Forsyth et al \(1990\)](#) as active tectonic adjustment along margin structures related to rapid sediment loading effects, whereas [Stephenson and Smolyaninova \(1999\)](#) postulated a localised tectonic mechanism associated with dynamic processes intrinsic to the lithosphere-asthenosphere boundary geometry along a rifted margin coupled with post-glacial rebound effects. The gravity, magnetic and seismicity characteristics of this segment of the CAM are similar to those of many known rifted passive continental margins in different regions of the world (e.g. [Vogt et al., 1998](#)).

The second segment of the CAM, the offshore Ellesmere Island-Alpha Ridge segment, is characterised by unusual and striking variability in potential field anomaly patterns (i.e. relatively positive to near-positive, linear to curvilinear gravity anomalies and magnetic highs and lows), which can be taken as related to widespread mafic volcanic and intrusive igneous rocks within the crust (e.g. [Grantz et al., 2011](#)), ‘underplated’ high density/high velocity lower crust and/or crustal basement highs together with thinner sedimentary cover. Aeromagnetic and gravity data in the transition zone between these contrasting domains of the CAM are analysed in detail in this paper.

3. Geology and tectonics of the study area

The geology and tectonics of the northeast CAM have been inferred from known onshore geology combined with the available onshore – offshore geophysical information (especially seismic and potential field data). It exhibits a complex geological and tectonic history that can be summarised simply as follows ([Balkwill, 1978](#); [Stephenson et al, 1987](#); [Trettin, 1989](#); [Trettin, 1991](#); [Forsyth et al, 1998](#); [Embry and Beauchamp, 2008](#) and references therein):

1. Formation of Franklinian Basin in the Early Palaeozoic; followed by deformation, magmatic intrusion and partial metamorphism of thick strata of carbonates, clastics and volcanics in the Silurian – Devonian associated with the Ellesmerian Orogeny.
2. Formation of the northeasterly elongate Sverdrup Basin by continental extension (as a rift-like basin) in the Late Carboniferous – Early Permian on the site of the

Ellesmerian orogenic belt and subsequent deposition of clastic and carbonate sediments, accompanied by Early Permian – Mid Jurassic thermal subsidence and continued deposition of thick sedimentary successions.

3. Continental rifting along the northwestern Sverdrup Basin margin in the Mid Jurassic – Early Cretaceous.
4. Seafloor spreading in Canada Basin, Alpha Ridge magmatism and much of the associated widespread episodic magmatic activity (resulting in the emplacement of mafic dykes, sills, flood basalts, thin lava flows and other volcanics in the Sverdrup Basin region) thought to have occurred in the Early-Mid Cretaceous.
5. Thermal subsidence of the area in the Late Cretaceous – Early Cenozoic, accompanied by deposition of thick sedimentary successions on the continental margin.
6. Uplift, folding and thrusting of the Sverdrup Basin (particularly its northeastern region of Ellesmere and Axel Heiberg islands) and other intramontane basins situated within the Ellesmerian orogenic belt, in the Eocene – Oligocene due to the impingement of Greenland on Ellesmere Island (Eurekan Orogeny) associated with seafloor spreading in the Labrador Sea and North Atlantic Ocean.
7. Formation of the present Canadian Arctic Shelf in the Neogene, and deposition of Neogene – Recent sediments (clastic wedge) constituting the Arctic Coastal Plain and its offshore equivalent.

The onshore Sverdrup Basin region of the study area contains up to 13 km thick Carboniferous to Palaeogene sedimentary strata (Balkwill, 1978) and, furthermore, displays widespread occurrences of magmatic rocks older and younger than the Carboniferous. Outcrops of magmatic and metamorphic rocks older than the Carboniferous (i.e. those related to the Ellesmerian orogenic events) are restricted to northwestern Ellesmere Island and northernmost Axel Heiberg Island (Okulitch, 1991; Trettin, 1991 and references therein; Figure 3). Devonian magmatic rocks (mostly granites, quartz monzonites and/or granodiorites), as well as Mesoproterozoic metamorphic rocks (predominantly amphibolites, gneisses and schists) occur around the Phillips Inlet area of the northwestern Ellesmere Island region (Figure 3). Devonian intrusive rocks (chiefly diorites, quartz diorites, tonalites), Neoproterozoic – Carboniferous volcanic rocks and the Neoproterozoic – Cambrian metamorphic rocks (mainly quartzites, slates and other metasediments of the Grant Land Formation) also occur on northernmost Axel Heiberg Island (Figure 3).

[Insert Figure 3 about here]

Magmatic rocks (mainly volcanic rocks, dykes, and mafic sills) younger than Carboniferous (mostly Cretaceous) are generally widespread in most regions of Ellesmere and Axel Heiberg islands, whereas Cretaceous mafic dykes and sills occur mainly on Ellef Ringnes and Amund Ringnes islands (Figure 3). Volcanic rocks (mainly flood basalts, thin lava flows and pyroclastics/tuffs) are almost entirely emplaced within the Late Albian – Cenomanian Strand Fiord Formation and Late Barremian – Aptian Isachsen Formation, whereas the mafic dykes and sills occur within most Mesozoic sedimentary units (e.g. Embry and Osadetz, 1988; Embry and Beauchamp, 2008; Figures 3 and 4). These volcanic and intrusive rocks are generally considered as part of the High Arctic Large Igneous Province (HALIP) (Ricketts et al., 1985; Embry and Osadetz, 1988; Buchan and Ernst, 2006; Døssing et al. 2013a, 2013b) and the causative mechanism that resulted in their episodic emplacement is widely ascribed to an Early Cretaceous mantle plume/hotspot centred in the Alpha Ridge area, which also emplaced the huge Alpha Ridge magmatic edifice (~ 30 km thick) in the contiguous Amerasia Basin of the Arctic Ocean (e.g. Embry and Beauchamp, 2008 and references therein). In addition, the Hansen Point Volcanics (HPV), consisting of a thick (~ 1000 m) sequence of lava flows and pyroclastics with intercalated clastic fluvial and marine sedimentary layers, occur on northwestern Ellesmere Island (Trettin and Parrish, 1987; Figure 3) and are of Late Cretaceous (88-94 Ma) (Embry and Osadetz, 1988; Richard et al., 2013; BGR, 2014) to Early Palaeogene (~ 64 Ma) age (Estrada and Henjes-Kunst, 2004; BGR, 2014). Salt diapirs (and other salt-cored intrusive structures/features) assigned to the Carboniferous Otto Fiord Formation are also widespread across the onshore Sverdrup Basin area and have in places penetrated the entire overlying, younger sedimentary successions/strata (Balkwill, 1978; Stephenson et al., 1992; Boutelier et al. 2011; Figure 3).

[Insert Figure 4 about here]

4. Datasets and methods

4.1. Aeromagnetic anomaly data

The digital aeromagnetic data used in this study were extracted from the new Circum-Arctic magnetic anomaly grid (CAMP-M) dataset compilations (Gaina et al., 2011; Saltus et al., 2011). The new CAMP-M compilation has a 2 km grid resolution, lower altitude (1 km), and hence better than previous magnetic anomaly grid compilation datasets such as the World Digital Magnetic Anomaly Map (WDMAM) with 3 arc-minute resolution (ca. 6 km) (Maus et al., 2007), GAMMA 5 magnetic anomaly data of the North Atlantic and Arctic (5 km resolution; Verhoef et al., 1996) and the 2 arc-minute global Earth Magnetic Anomaly Grid

(EMAG2) (ca. 4 km resolution; [Maus et al., 2009](#)). Structures and causative geological bodies exhibiting short to long wavelength (high to low wavenumber) magnetic anomalies could be delineated and mapped from it, since it has a 2 x 2 km grid resolution and spherical harmonics degree 130 (i.e. ~ 333 km wavelength) with the MF6 lithospheric satellite-derived magnetic anomaly model ([Gaina et al., 2011](#)). This implies that the resolution of the magnetic data is appropriate for basin-scale to regional-scale geological and tectonic studies.

The extracted aeromagnetic (total magnetic intensity, TMI) data of the area were re-gridded at the same scale employing a bi-directional gridding method, which uses Akima splines to interpolate data readings down-lines and across-lines to determine the values at the grid nodes ([Akima, 1970](#); [Geosoft Inc., 2008, 2012](#)), and subsequently re-projected using the Universal Polar Stereographic North coordinate system and geo-referenced to the World Geodetic System 1984 (WGS84) ellipsoid datum.

The study area is located near the magnetic north pole; nevertheless, it is helpful to apply a reduction to pole (RTP) transformation ([Dobrin and Savit, 1988](#); [Sheriff, 2002](#)) in order to avoid any shift in the magnetic anomaly positions. Hence, the TMI grid data were transformed using the RTP filter, and the Butterworth low-pass filter applied simultaneously to eliminate short-wavelength (high-wavenumber) components associated with noise present in the data. Geomagnetic inclination, declination and amplitude corrections of 88.50°, -62.41°, and 20, respectively, are the RTP filter parameters used, whereas the parameters of Butterworth low-pass filter are 5000 m cut-off wavelength and filter order of 8. The 88.50° and -62.41° are mean values of the geomagnetic inclination and declination, respectively calculated for the entire study area based on the IGRF-11 model for year 2010 as adopted by the International Association of Geomagnetism and Aeronomy (IAGA), using the National Geophysical Data Centre (NGDC) Geomagnetic Calculator ([NOAA/NGDC, 2010](#)). The RTP-TMI anomaly map of the area ([Figure 5](#)) produced has precise magnetisation directions, ambient magnetic field and shows relatively minor change in shapes and positions of magnetic anomalies.

[Insert Figure 5 about here]

4.1.1. Aeromagnetic anomaly enhancement

The first vertical derivative (FVD), second vertical derivative (SVD) ([Dobrin and Savit, 1988](#); [Telford et al., 1998](#); [Cooper and Cowan, 2004](#)), total horizontal derivative (THD)

(Cordell and Grauch, 1985; Phillips, 1998) and analytic signal (AS) (Roest et al., 1992; Macleod et al., 1993; IGC, 1996; Wijins et al., 2005; GETECH, 2007) enhancement methods were applied to the RTP-TMI anomaly data grid in the Fourier domain using appropriate filters and parameters (Geosoft Inc. 2011) in order to delineate and enhance/accentuate the edges of shorter-wavelength anomalies (shallow magnetic sources) associated with geological bodies (e.g. flood basalts, thin lava flows, dykes, sills) and structures in the area (Anudu et al., 2014). They were also utilised in the identification and delineation of magnetic domains related to major causative geological and tectonic features across the area. The resultant edge enhanced (derivative) magnetic anomaly maps with various identified magnetic domains superimposed are presented in Figures 6 – 9.

[Insert Figures 6 – 9 about here]

Additionally, the RTP-TMI anomaly data grid was also subjected to a pseudogravity (PSG) transformation in the Fourier domain (Blakely, 1996) using the pseudogravity (PSG) filter in order to image and enhance longer-wavelength anomalies related to large, deep, magnetised geological sources. Generally, pseudogravity highs indicate presence of deep-seated positively magnetised sources and the lows indicate absence of deep-seated magnetised sources. The resulting PSG anomaly map (Figure 10) was, subsequently, upward continued by 25 km to highlight further more deep-seated (regional), crustal-scale features (Figure 11). In conducting this transformation, several computed PSG filter parameters together with assumed induced magnetisation only in the ambient field direction were used. The assumption of magnetisation by induction only is justified because there was no smearing of anomalies on the RTP-TMI anomaly map (Figure 5) and maxima (peaks) on the RTP-TMI anomaly map occur at the same positions as on the AS-TMI anomaly map (e.g. Milligan and Gunn, 1997; Figure 9). Comparison of the PSG anomaly maps (Figures 10 and 11) with the gravity anomaly map of the area (Figure 12) suggests that most of the observed anomalies on these maps are likely to be caused by the same or similar crustal geological bodies and tectonic features.

[Insert Figures 10 and 11 about here]

4.2. Gravity anomaly data

The gravity (Bouguer onshore, Free-Air offshore) datasets used in this study are mainly from the 1961 to 1987 gravity data compilations that were acquired during several regional (large-scale) gravity surveys conducted across the Arctic Canada region by the Geological Survey of Canada (GSC). The gravity datasets were provided by the Geophysical Data Centre of

GSC Ottawa and these datasets, consisting of about 5630 gravity data points, are generally unevenly distributed (c. 2 – 10 km average spacing) across the study area. According to the GSC, all the gravity measurements were tied to the Canadian Gravity Standardisation Network (CGSN) and later subjected to requisite gravity data reductions such as instrumental drift, latitude, Free-Air, Bouguer and terrain corrections where necessary/appropriate. The accuracy of the gravity anomaly data is estimated to be within 3 mGal (e.g. [Stephenson and Ricketts, 1990](#)). The resulting gravity anomaly data, which chiefly reflect the effects caused by density variations associated with water depths, sediment properties, crustal thicknesses and composition, and mantle properties were projected using the Polar Stereographic North coordinate system and geo-referenced to the World Geodetic System 1984 (WGS84) ellipsoid datum and, subsequently, interpolated to a regularly spaced grid of 1.5 km using the minimum curvature method ([Briggs, 1974](#)). The gravity (Bouguer onshore, Free-Air offshore) anomaly map generated is presented in [Figure 12](#) and its resolution is adequate for regional (large-scale) and relatively detailed gravity studies.

[Insert Figure 12 about here]

4.2.1 Gravity anomaly isolation and enhancement

4.2.1.1. Regional-residual gravity anomaly separation

Because the gravity anomalies represent the cumulative effects of all gravitational attraction caused by the lateral variations in densities of subsurface (shallow- and deep-seated) geological bodies, it may be advantageous to decompose them first into regional (large-scale) and residual (local/small-scale) components, a process commonly referred to as regional-residual separation ([Telford et al., 1990](#); [Sheriff, 2002](#)). In the present study, regional-residual separation was applied to the gridded gravity anomaly data employing the wavelength filtering method, which is the most common, flexible and efficient analytical numerical method for conducting regional-residual separation. It has higher accuracy than the polynomial fitting method ([Dobrin and Savit, 1988](#); [Jacoby and Smilde, 2009](#)). The wavelength filtering was performed using the Gaussian regional-residual filter.

The gridded gravity anomaly data were transformed to the spectral domain (Fast Fourier Transform) and then subjected to filtering employing the Gaussian regional-residual filter with a 200 km cut-off wavelength to obtain the residual ([Figure 13](#)) and regional ([Figure 14](#)) anomalies. This Gaussian filter parameter was chosen after careful and rigorous evaluations of various residual anomalies generated using several cut-off wavelengths as well as based on

the gravity analysis rule expressed as $Z_c \approx \lambda / 6$, where λ is limiting wavelength of causative body and Z_c is its depth (Hinze et al., 2013).

The resulting residual gravity anomaly map (Figure 13) shows good correlation with the known surface geology (Figure 3) and edge enhanced (derivative) magnetic anomaly maps (Figures 6 – 9); thus indicating that it is geologically plausible ('appropriate and acceptable'). It gives prominence to density contrasts in upper-crustal regions and, hence, greatly emphasises the anomalies of interest, which are related to shallow causative geological and tectonic features such as flood basalts, faults, and regional structures such as the Princess Margaret Arch (PMA) and Cornwall Arch (CA)(Figure 3). Many of these features were barely perceptible on the original gravity anomaly map (Figure 12). In contrast, the regional gravity map (Figure 14) emphasises the long-wavelength (low wavenumber) anomalies associated with large, deeper (regional) gravity sources (e.g. crustal and crust-mantle interface structures) by removing undesirable residual anomaly components and noise.

[Insert Figures 13 and 14 about here]

4.2.1.2. Gravity anomaly enhancement

Three enhancement (derivative) methods, namely First Vertical Derivative (FVD; Dobrin and Savit, 1988; Telford et al., 1998; Cooper and Cowan, 2004), Total Horizontal Derivative (THD; Cordell and Grauch, 1985; Phillips, 1998) and tilt derivative (TD; Miller and Singh, 1994; Verduzco et al., 2004) were applied to the gravity anomaly grid to recognise and accentuate the edges of anomalies (gravity causative sources) related to shallow geological features such as geological contacts, crustal basement structures and other structural fabric, which is widely used for structural mapping. The resultant edge enhanced (derivative) gravity anomaly maps are shown in Figures 15 – 17.

[Insert Figures 15 – 17 about here]

5. Results

5.1. Magnetic domains and geology

Magnetic domains and/or their boundaries are significant in geological studies (e.g. mapping litho-tectonic terrane boundaries), as well as important to mineral and petroleum exploration as potential zones of intense deformation, magmatism and fluid/heat flows (Saltus et al. 1997). The RTP-TMI anomaly map and other derived edge enhanced (derivative) magnetic anomaly maps (FVD-RTP-TMI, SVD-RTP-TMI, THD-RTP-TMI, AS-TMI) were used in the

recognition and delineation of different magnetic domains and their associated geological bodies/structures across the study area (Figures 5 – 9). The approach employed involves the identification of those areas with distinctive or clearly-defined anomaly patterns and tectonic fabrics on these magnetic anomaly maps (e.g. Parasnis, 1986; Saltus et al. 1997; Telford et al., 1998; Anudu et al., 2014) and their explanation in terms of possible causative structures (e.g. Reeves, 2005; Anudu et al., 2014). Additionally, many known exposed magmatic rock bodies (e.g. HPVs, flood basalts) and other surface geological/tectonic features were correlated with their associated anomalies on the various magnetic anomaly maps. Five (5) main magnetic domains (A, B, C, D and E) are delineated across the study area (Figures 5 – 9) and the major distinctive magnetic anomaly patterns or attributes that were used in doing so are anomaly amplitudes, wavelengths (wavenumbers), gradients and dimensions (e.g. linear, curvilinear, broad, etc.) as well as geological information and geodynamic setting. Each defined/mapped magnetic domain exhibits strikingly similar anomaly pattern or attributes, geological and tectonic trends distinguishing it from adjoining domains.

Domain A occupies the northern part of the study area and is situated within the Arctic Ocean region (Figures 5 – 9). It exhibits relatively chaotic, sub-linear to linear, broad, medium- to long-wavelength (moderate- to low-wavenumber) magnetic anomalies with very high to very low amplitudes and is associated with the southern flank of the Alpha Ridge magmatic complex (Figure 5). Similar types of magnetic anomaly patterns have been observed across the entire Alpha Ridge region (Figure 2b), as well as over the contiguous Mendeleev Ridge (e.g. Saltus et al., 2011). Domain A is sub-divided into two sub-domains A1 and A2 primarily based on the magnetic anomaly amplitudes and wavelengths. Sub-domain A1 is characterised by very high to moderately high (positive) amplitude, broad longer-wavelength anomalies and is the larger of the two sub-domains, while sub-domain A2 is characterised by low to very low (negative) amplitude, medium-wavelength anomalies with narrower anomaly widths. Sub-domains A1 and A2 display several forms of regular to irregular ‘ridge- and trough-like’ anomaly patterns of various dimensions with A1 being ridge-like and A2 as trough-like features on most maps, especially the RTP-TMI map (Figure 5). The observed ridge- and trough-like geological features are speculated to have been developed along pre-existing structures or weak zones in the crustal basement of Alpha Ridge region prior to major continental extension, later being reactivated and accentuated mainly by extensional tectonic movements occurring after the cessation of the HALIP magmatic activities. This interpretation agrees with Bruvoll et al (2012) according to whom the horst and graben

topography across the northwestern Alpha Ridge developed by extensional faulting after the end of magmatic activities. Sub-domain A1 magnetic anomalies are 10 to 100 km wide, 15 to 250 km long and trend predominantly in a NE-SW direction with minor N-S and ESE-WNW strikes, whereas those of sub-domain A2 are up to 70 km wide, 7 to 110 km long and show major NE-SW and ESE-WNW trends on the RTP-TMI anomaly map (Figure 5). Published seismic reflection studies (Jackson, 1985; Jokat, 2003; Bruvoll et al., 2010, 2012) show that acoustic basement depths (equivalently, thickness of sediments) over the Alpha Ridge area vary from 0.5 to about 2.7 km; hence sub-domain A2 with low amplitude anomalies (-155 to -250 nT) on the RTP-TMI anomaly map (Figure 5) is likely related to several localised, shallow crustal basement trough- or graben-like features present in the Alpha Ridge region. The predominance of widespread, broad, high (positive) magnetic anomaly amplitudes (up to 1380 nT) in the sub-domain A1 together with available seismically mapped crustal velocity models (e.g. Forsyth et al., 1986a, 1986b; Weber, 1990; Jokat, 2003; Piskarev, 2004; Funck et al., 2011; Bruvoll et al., 2012) coupled with geochemical and petrological results from rock core samples recovered from the Alpha Ridge (e.g. Van Wagoner and Robinson, 1985; Jokat et al., 1999; Mühe and Jokat, 1999) suggests the presence of massive and extensive volume of mafic magmatic rocks, especially basalts. Domain A also displays tectonic and crustal magnetic anomaly features typical of volcanic margin provinces with a weakened, highly extended continental crust (e.g. Bruvoll, et al., 2012) or a continental crust that has been highly stretched, attenuated and intruded due to rifting, excessive volcanism and other magmatic activities usually associated with mantle plumes. Previous magnetic study conducted very close to this domain by Døssing et al. (2013a) reveals that at least the segment of Alpha Ridge nearest to Canadian- Greenland margins together with area adjacent to Lomonosov Ridge is underlain by continental crust attenuated prior to the emplacement of the volcanic edifice (magmatic complex) based on the interpretation of numerous, linear to sub-linear aeromagnetic anomalies observed across the region. Edges of the anomalies within domain A, especially on the THD-RTP-TMI anomaly map (Figure 8), have sharp and well-defined maxima and hence accurately delineate and map the causative volcanic rocks of the Alpha Ridge igneous complex. The magnetic anomaly maps also reveal that the massive and extensive, mafic HALIP volcanic rocks of the offshore Alpha Ridge overlaps with the northwestern Ellesmere Island Arctic margin to the east and also extend up to latitude 81° 10'N, longitude 110°W and latitude 81° 10'N, longitude 103°W in the western part of the study area (Figures 5 – 9).

Domain B consists of two sub-domains, namely B1 and B2 (Figures 5 – 9). Sub-domain B1 occupies the western and west-central part of the study area, which coincides with the Canadian Arctic shelf region. The anomalies are essentially NE-SW and NW-SE oriented with some subordinate ENE-WSW trends (Figure 5). It shows distinctive magnetic anomaly characteristics, being composed of medium-wavelength, quasi-linear to curvilinear anomalies with moderately high to low amplitudes which distinguishes it from the contiguous domain A (Alpha Ridge region) to the north and domain D to the south (Figure 5). It lacks magnetic anomaly and crustal character (magnetic expressions) typical of most ocean basins of the world. Previous seismic refraction studies (Argyle and Forsyth, 1994; Forsyth et al, 1998; Funck et al., 2011) within sub-domain B1 reveal shallow Moho depths (c. 20 – 26 km deep) and a thin/attenuated continental crust (c. 14 – 21 km thick). In addition, the anomaly patterns and wavelengths exhibited in sub-domain B1 are strikingly similar to that of the continental margin of Gulf of Mexico ocean basin (NAMAG, 2002) and other marginal sea basins (e.g. South China Sea), which is underlain by hyper-extended continental crust (Harry, 2008) or foundered continental crust (Zhetan et al., 1981). Hence, B1 is interpreted as a marginal oceanic basin region underlain by attenuated continental crust with relatively thick sedimentary cover. An important observation about sub-domain B1, especially on the RTP-TMI, THD-RTP-TMI and AS-TMI anomaly maps (Figure 5, 8 and 9) is the absence of high amplitude (positive), short-wavelength (high wavenumber) anomalies usually related to magmatic intrusions (e.g. flood basalts, dykes, sills); this might indicate that the opening and development of the marginal oceanic basin probably occurred after the Alpha Ridge magmatism. Sub-domain B2 occupies the southern and southwestern parts of the study area and covers mainly Amund Ringnes Island and adjoining areas (Figures 5 – 9). It displays major NW-SE, NE-SW, ESE-WNW and ENE-WSE trends on the magnetic anomaly maps. On the RTP-TMI map, sub-domain B2 exhibits anomaly patterns composed of linear to sub-linear and sub-circular, medium-wavelength (moderate-wavenumber) magnetic anomalies with relatively high to low amplitudes (Figure 5) and such anomalies are due to underlying magmatic intrusions imaged on the edge enhanced (derivative) magnetic anomaly maps (Figures 6 – 9), as well as salt diapirs and diapiric structures (containing evaporites and magmatic bodies) concealed within the sedimentary succession (e.g. Stephenson et al., 1992). This interpretation is consistent with the geology of the area (Figure 3). The broad, intermediate (positive) medium-wavelength magnetic anomalies with smooth character and low amplitudes around the southeastern and southwestern areas of sub-domain B2 could be

due to near-surface accumulations of diagenetic magnetic minerals associated with hydrocarbon-related chemical reactions, or cultural iron contamination and authigenic alterations in sedimentary rocks, possibly caused by hydrocarbon migration into and along the underlying geological or tectonic structures in the area (e.g. [Costanzo-Alvarez et al., 2000](#); [Aldana et al., 2003](#)). Some hydrocarbon fields (e.g. Kristoffer, Thor, Jackson bay, Cape Allison, among others) have been discovered around the Kristoffer Bay area abutting Ellef Ringnes Island to the southwest ([Embry and Beauchamp, 2008](#)).

Domain C lies in the northwestern Ellesmere Island region situated within latitude 82° 50'N, longitude 91° 25'W and latitude 81°N, longitude 85°W at the eastern margin of the study area ([Figures 5 – 9](#)). It is characterised by high to low amplitude, short- to medium-wavelength anomalies with linear and circular to elliptical patterns, and is associated with occurrences of the HPVs, dykes, pyroclastic and clastic sedimentary rocks on northwestern Ellesmere Island-Alpha Ridge margin ([Trettin and Parrish, 1987](#); [Embry and Osadetz, 1988](#); [Estrada et al., 2006](#); [Figure 5](#)). The tectonic/structural trends on the magnetic anomaly maps are predominantly NE-SW and ENE-WSW. In addition, the conspicuous and well-defined circular to elliptical magnetic anomaly observed at latitude 81° 30'N, longitude 91° W (around the Emma Fiord –Audhild Bay area in the northeastern Nansen Sound entrance region), with amplitude in excess of 235 nT and wavelength of about 50 km on the RTP-TMI anomaly map ([Figure 5](#)), delineates the HPV. These interpretations are consistent with the established geology of the area ([Figure 3](#)).

Domain D occupies the southeastern, southcentral and southwestern parts of the study area ([Figures 5 – 9](#)). It covers most of the Axel Heiberg Island, Nansen Sound, Sverdrup Channel, Meighen Island, Peary Channel and Ellef Ringnes Island regions situated with the east-central Sverdrup Basin (also known as the “Sverdrup Basin Magmatic Province”) ([Williamson et al., 2011](#)) of the Queen Elizabeth islands. It exhibits distinct groups of parallel, linear to sub-linear, short- to medium-wavelength magnetic anomalies with high (positive) amplitudes associated mainly with widespread dyke swarms (e.g. [Døssing et al. 2013a](#)), as well as several broad non-linear to near-circular high amplitude anomalies due to sills, flood basalts, basaltic lava flows and volcanic centres ([Figures 5 – 9](#)). Domain D can be subdivided into two sub-domains, D1 and D2, mainly on the basis of the orientations of these swarm dykes ([Figures 6 – 9](#)). In sub-domain D1, dyke swarms (up to 250 km long) trend

predominantly in the NW-SE direction with minor ESE-WNW trends and occupy mainly the central region of the Axel Heiberg Island, whereas those in sub-domain D2 are essentially NE-SW and N-S oriented with subordinate ENE-WSW orientation and cover most regions of the Sverdrup Basin with the exception of the central Axel Heiberg Island area. The various trends displayed by these dyke swarms are likely to have resulted from the combined effects of intraplate deformation caused by the relative tectonic movements of the North American plate (Buchan and Ernst, 2006), tectonic deformation due to the Eureka Orogeny (Jackson and Halls, 1988; Stephenson and Ricketts, 1990), compressive stress fields, pre-existing structures/trends, different episodes of magmatism (volcanism) and associated tectonism which occurred in most Queen Elizabeth islands of the northern Canadian Arctic islands, especially during the Cretaceous to Palaeogene. The prominent broad and extensive, non-linear to relatively circular magnetic anomaly features with high (positive) amplitudes observed around latitude 79° 20'N, longitude 92°W as well as latitude 81° 20'N, longitude 95°W at the west-central and northwestern Axel Heiberg Island in sub-domain D1 are associated with the flood basalts of the late Albian – Cenomanian Strand Fiord Formation (Ricketts et al., 1985; Embry and Osadetz, 1988) and the basalt lava flows and sills of the late Barremian – Aptian Isachsen Formation (Embry and Osadetz, 1988; Williamson et al., 2011; Figures 5 – 9). Ricketts et al (1985) reported that the thickness of the Strand Fiord Formation basalts is about 100 to 137 m around the Strand Bay Fiord – Expedition Fiord area (west-central Axel Heiberg Island) and over 789 m in northwestern Axel Heiberg Island), whereas Embry and Osadetz (1988) stated that the Isachsen Formation basalt flows are up to 220 m thick in the same area. The presence of these extensive, thick intra-sedimentary flood basalts and other associated magmatic intrusions (chiefly mafic sills, dykes) is a contributory causative factor to the 'West Axel Heiberg Gravity High' observed on gravity anomaly map of the area (Oakey and Stephenson, 2008; Figure 12), since these magmatic rocks are mafic in composition and therefore dense. Pockets of circular to near-circular, positive short-wavelength magnetic anomalies observed within sub-domain D2 on northern Axel Heiberg Island (Figures 5 – 9) are due to outcropping and near-surface, Devonian dioritic rock bodies (e.g. diorite, quartz diorite) of the Franklinian basement (Figure 3). The smaller, non-linear to near-circular magnetic anomaly features having high (positive) amplitudes widely observed around the central Ellef Ringnes Island region are interpreted to be due to mafic sills exhibiting saucer-shaped structures (i.e. saucer-shaped mafic sills) (e.g. Evenchick et al., 2015), although some of them may be associated with mafic volcanic rocks and dykes. This

interpretation agrees with field geological studies (e.g. [Evenchick et al., 2015](#)) and with [Stott \(1969\)](#) who interpreted several outcrops of circular structures around this area to be largely composed of diabase and gabbro.

Domain E is a distinct, narrow and elongated magnetic domain. It begins from northern Ellef Ringnes Island in the southwest, extends eastwards to southern Meighen Island and then northwards through the marginal areas of northwestern Axel Heiberg Island ([Figures 5 – 9](#)). Domain E, together with the portion of sub-domain D2 situated on northcentral Ellef Ringnes Island, is characterised by major sub-linear to curvilinear NE-SW, E-W to N-S trending, moderate (positive) amplitude, medium- to short-wavelength anomalies. Such magnetic anomaly patterns are associated with volcanic rocks (mainly basaltic lava flows), mafic sills and dykes plus other magmatic intrusions emplaced in sedimentary strata of the Sverdrup Basin in this area ([Figure 3](#)). The magnetic domain E together with some portions of sub-domain D2 on north-central Ellef Ringnes Island region coincide with the axis of several distinct gravity anomaly highs ([Figure 12](#); see section 5.3 for detailed discussion) which [Oakey and Stephenson \(2008\)](#) ascribed to mafic sills and dykes.

5.2. Pseudo-gravity anomalies and geology

The Pseudogravity (PSG) anomaly maps ([Figures 10 and 11](#)) reveal the magnetic character of the underlying crustal rocks (e.g. [Hinze et al., 2013](#)) across the study area. They highlight the long wavelength (regional) anomalies associated with deeper and broader (regional) geological causative bodies likely attributable to Precambrian crustal basement rocks/structures beneath the Sverdrup Basin, Canadian Arctic Shelf and Alpha Ridge regions as well as those caused by the intra-basement igneous rocks in the Alpha Ridge area. These deep-seated, regional (long wavelength) anomalies are generally difficult to recognise on the original RTP-TMI anomaly map ([Figure 5](#)). They also reveal that the crustal rock magnetisation probably decreases from the offshore Alpha Ridge magmatic complex to the Sverdrup Basin region. That is, the crustal rocks beneath the Alpha Ridge, Canadian Arctic Shelf and Sverdrup Basin exhibit high magnetisation, medium magnetisation and low magnetisation, respectively. The high magnetisation of the Alpha Ridge is due to the presence of numerous, mafic dense volcanic and intrusive magmatic bodies in the upper crust, whereas the low magnetisation in the Sverdrup Basin region is suggestive that the underlying Franklinian crustal basement is probably less magnetic. Low amplitude, negative (< -0.0018 mGal) long wavelength anomalies with dominantly NE-SW and NW-SE trends

characterised the Sverdrup Basin (especially in the southern Axel Heiberg Island area). Moderate amplitude (-0.0018 to 0.0054 mGal) anomalies trending mainly NW-SE and NE-SW are observed within the offshore Canadian Arctic Shelf area. High to moderate amplitude, medium to long-wavelength anomalies striking predominantly NE-SW and ENE-WSW with minor NW-SE and WNW-ESE trends occur across the Alpha Ridge region. On the upward continued 25 km pseudogravity anomaly map (Figure 11), the observed positive anomalies strongly correlate with the voluminous, mafic volcanic and intrusive rocks (i.e. HALIP) of the offshore Alpha Ridge magmatic complex and may be due to the underlying intruded thick crust (with high magnetic character), whereas the strong negative low anomalies present over the southern Axel Heiberg Island and adjoining southern Ellesmere Island are likely to be related to thick sedimentary successions and deep-seated, weakly magnetised thicker continental crust.

5.3. Gravity anomalies and geology

The gravity anomaly map expresses the lateral variations in the density of the underlying geological bodies (Figure 12) and thus gives a first order overview of the character of the subsurface geology, both shallow- and deep-seated, across the study area. On the gravity anomaly map (Figure 12) and its residual anomaly map (Figure 13) and edge enhanced anomaly maps (Figures 15 – 17), several prominent anomalies are marked to aid in their identification and interpretation with regards to their probable causative geological bodies and/tectonic features.

The gravity anomaly field around the Canadian Arctic Shelf region of the study area (labelled H1 and referred to as ‘Canadian Arctic Shelf-Slope High’; Figures 12 – 14) is characterised by distinct, large-scale (regional) NE-SW and E -W trending elliptical gravity highs (in excess of 24 mGal), as well as high gradients (Figures 15 – 17), with axes spatially coincident and nearly parallel to the shelf-slope areas (c. 454 – 1900 m bathymetric depth contours; Figure 1). Similar anomaly patterns are present along the entire Canadian Arctic shelf (e.g. Forsyth et al., 1990; Vogt et al., 1998; Figure 2a) and have been previously interpreted to be related to Moho ridge structure (Sobczak, 1975), variations in density of the mantle beneath the thin continental crust (Sobczak et al., 1986) and thick, young (Neogene) isostatically undercompensated sedimentary loads and edge effects (Sobczak, 1975; Sobczak et al., 1986; Forsyth et al., 1990; Stephenson et al., 1994). An alternative interpretation for the causative source(s) of these prominent features is that they result from the combined effects of a thick

continental crust adjacent to attenuated continental crust, magmatic underplating (i.e., ‘underplated’ high density/high velocity lower crust), uplifted crustal basement and large bathymetric gradient at the shelf-slope regions or edge effects. A thick, young (Neogene) isostatically undercompensated sedimentary succession is a contributory factor to these anomalies only in the offshore western region of the study area where the ‘Northeastern Canadian Arctic Marginal Basin’ (NECAMB) (Figure 18) has been delineated and mapped.

The localised, conspicuous broad circular to elliptical gravity high (> 24 mGal; Figures 12 – 14) with high gravity gradient (Figures 15 – 17), labelled H2, around the Emma Fiord - Audhild Bay area in the northeastern Nansen Sound entrance and northwestern Ellesmere Island marginal region (at latitude 81° 30’N, longitude 91° W; named here as ‘Northeast Nansen Sound high’) is due to the outcropping and near-surface, large mafic volcanic complex, generally referred to as Hansen Point Volcanics (HPVs), together with other associated magmatic intrusions (Figure 18). This prominent feature also exhibits a well-defined circular to elliptical magnetic high (in excess of 235 nT) (Figure 5) and therefore its interpretation is consistent with the field geology of the area (Figure 3).

The NW-SE elongated gravity high H3 (Figures 12 – 17) observed within and around the northern edge of Axel Heiberg Island coincides with the northern portion of the Princess Margaret Arch (PMA). It is attributed to the combined effect of magmatic intrusions, uplifted Neoproterozoic – Cambrian metasedimentary basement and near-surface Devonian dioritic rock bodies of the Franklinian basement. It is widely known that volcanic rocks, metasedimentary rocks and dioritic rocks outcrop in this region; thus, this interpretation is in good agreement with the established geology of the area (Figure 3). The striking broad and prominent NW-SE gravity anomaly high, H4, (Figures 15 – 17) observed over the Amund Ringnes Island region coincides with the Cornwall Arch (CA) with its northern segment occurring over several large magmatic intrusions magnetically mapped in the present study (Figures 5 – 9 and 18). Stephenson and Ricketts (1990) and Stephenson et al. (1990) interpreted the CA and PMA to be associated with large scale (regional) crustal folding. This anomaly is here interpreted to be due to the combined effect of high density magmatic intrusions emplaced within the relatively thin sedimentary successions, uplifted shallow crustal basement rocks, crustal folding and uplifted, high density mantle bodies.

The remarkable, broad N-S to NNE-SSW trending gravity highs (labelled H5) and NE-SW striking gravity high (labelled H6) with steep-gradients plus anomaly amplitudes up to 24 mGal situated northwest coast of Axel Heiberg and Ellesmere islands, respectively, as well as the NW – SE oriented gravity highs around the Sverdrup Channel (labelled H7) and Peary Channel area (labelled H8) (Figures 12 – 13 and 15 – 17) are coincident with numerous high amplitude (positive), short-wavelength magnetic anomalies in the magnetic anomaly map (Figure 5). These anomalies are interpreted to be primarily associated with numerous mafic magmatic intrusions (mainly volcanic rocks and mafic sills), which have been magnetically identified and mapped in this present study (Figures 5 – 9 and 18). However, the gravity anomaly highs (H5 – H7) may also be related to uplifted mantle bodies and crustal basement highs, since they are still present on the regional gravity anomaly map (Figure 14).

The conspicuous, large-scale gravity high (> 15 mGal) (Figures 12 – 14) with high gradients (Figures 15 – 17) and exhibiting a circular-like anomaly pattern observed on northcentral Ellef Ringnes Island (labelled H9) coincides with known occurrences of numerous, shallow mafic magmatic intrusions (mainly volcanic rocks and saucer-shaped sills) mapped geologically in field (Evenchick et al., 2015; Figure 3) and well imaged from magnetic data using edge enhancement (derivative) approach (Figures 5 – 9 and 18). This anomaly is also prominent on the regional gravity anomaly map (Figure 14) where it exhibits a near-circular anomaly shape, an indication that it is also (partly) caused by a larger and deeper or deep-seated geological body. Thus H9 is attributed to dense, mafic magmatic intrusions, shallow crustal basement highs and/or uplifted, dense upper mantle bodies (including Moho shallowing).

The prominent, broad (extensive) NW-SE oriented gravity low, L1, with anomaly amplitudes in excess of -40 mGal over southern Axel Heiberg Island on the gravity anomaly maps (Figures 12 – 14) does not have any coincident magnetic expression on the magnetic anomaly map (Figure 5) and, therefore, it is primarily attributed to the combined effects of Eurekaan crustal thickening and very thick (up to 13 km), low-density sedimentary cover. This interpretation is in good agreement with previous gravity studies (e.g. Oakey and Stephenson, 2008). It may also be related to crustal thickening in response to isostatic compensation of the broad, mountainous (more than 2000 m high) Axel Heiberg Island region (Figure 1). L1 is bound by striking narrow and elongated zones of steep gravity gradient to the southwest and northeast (Figures 12 – 17), consistent with the locations of two prominent regional-scale

thrust faults identified on the magnetic anomaly maps (Figures 5 – 9) that were mapped and named the Stolz Thrust fault (F1) and “South Strand Bay Fault” (F2) as shown in Figure 18. Additionally, the broad NE-SW trending gravity anomaly low, labelled L2, (Figures 12 – 16) observed on Ellesmere Island corresponds to the southwestern segment of the high topography of the Grantland Uplift (e.g. Stephenson and Ricketts, 1990; Oakey and Stephenson, 2008). Gravity lows over the entire Grantland Uplift area of Ellesmere Island have been interpreted by Stephenson and Ricketts (1990) and Oakey and Stephenson (2008) to be due to isostatically compensated thickened crust.

The regional gravity anomaly map reveals several prominent, large-scale (regional) deeper compressional tectonic structures with wavelengths in excess of 160 km around the southeastern region of the study area (Figure 14) widely affected by the Eurekan Orogeny. These tectonic structures (probably indicative of crustal folding) are hundreds of kilometres in length (100 – 350 km long) and consist of five anticlinal and another five synclinal structures with most of them plunging southeastwards (Figure 14). The separation between these ten sub-parallel subsurface tectonic structures is approximately 50 km, similar to undulating Moho topography recognised on regional seismic refraction results acquired within the region west of Amund Ringnes Island (Forsyth et al, 1979). Almost all of them are previously unknown or unrecognised. Two of the anticlinal structures delineated coincide with the actual positions of the well-known, large-scale Eurekan structural elements: the Princess Margaret Arch (PMA) and Cornwall Arch (CA). The PMA and CA were interpreted from regional seismic refraction studies by Forsyth et al (1979) and from regional gravity data analysis by Stephenson and Ricketts (1990) and Stephenson et al. (1990) to be due to crustal warping or folding.

6.0. Discussion

6.1. Mapping magmatic intrusions

The RTP-TMI anomaly data and their derivatives were utilised in the identification, delineation and mapping of magmatic intrusions (volcanic rocks, sills and dykes), faults and their areal extents across the study area (Figures 5 – 9), since they highlight and greatly enhance both the conspicuous and subtle high amplitude short-wavelength anomalies associated with these surface to near-surface rock bodies/features.

The ridges and margins of the numerous, high amplitude anomalies on all the above-mentioned magnetic anomaly maps (Figures 5 – 9), which represent the edges of various underlying magnetic causative geological bodies (particularly magmatic intrusions) within the onshore Sverdrup Basin were precisely identified and digitised on-screen. The resultant geological features from these maps were subsequently integrated to produce a new, more comprehensive magmatic intrusion distribution map (Figure 18). It reveals that extensive magmatic intrusions (mainly volcanic rocks and sills) occur across the northwestern and west-central Axel Heiberg Island regions, northwestern Ellesmere Island region and eastern Ellef Ringnes Island area, as well as areas situated within the Sverdrup and Peary channels. Furthermore, large-scale dykes occupy the central Axel Heiberg Island and northwestern Ellef Ringnes Island region (Figure 18). Additionally, two prominent regional geological faults (more than 100 km long) identified and mapped at the southern Axel Heiberg Island are the Stolz Thrust Fault (labelled F1) and another fault (labelled F2) named here the ‘South Strand Bay Fault’ (Figure 18); both faults trend NW-SE and are represented on the magnetic anomaly maps by abrupt truncations of linear anomalies and coincident high gradients (Figures 5 – 9).

[Insert Figure 18 about here]

The numerous circular to curvilinear anomaly bodies as well as several ‘sheet-like’ anomaly features are identified as volcanic rocks and sills, since circular, curvilinear and ‘sheet-like’ magnetic causative geological features are frequently associated with mafic intrusions and basaltic flows (Parasnis, 1986). However, most of the narrow elongated linear anomaly bodies are defined as dykes because most long, narrow magnetic geological features are very often due to dykes (Parasnis, 1986). This interpretation is consistent with surface geological mapping and published field geological studies (Figure 3). Several basalts (> 789 m thick) and basaltic lava flows (up to 220 m thick) with interbedded pyroclastics have been mapped within the late Albian – Cenomanian Strand Fiord Formation (Ricketts et al., 1985) and late Barremian – Aptian Isachsen Formation (Embry and Osadetz, 1988) exposed on northwestern Axel Heiberg Island. Basalts of the Strand Fiord Formation (up to 250 m thick; Ricketts et al., 1985; Embry and Osadetz, 1988) as well as diabase sills and dykes (Embry and Osadetz, 1988; Embry, 1991; Stephenson et al., 1992) outcrop in the Strand Bay area, west-central Axel Heiberg Island. Volcanic rocks, particularly basalts, lava flows and pyroclastics, are exposed close to the northeastern Nansen Sound entrance (HPV; c. 1000 m thick) and on the northwestern Ellesmere Island margin (c. 645 m thick) (Trettin and Parrish, 1987; Embry and Osadetz, 1988; Okulitch, 1991). Furthermore, gabbro dykes, sills, lava flows and tuffs are

also encountered across northern and eastern Amund Ringnes Island (Balkwill, 1983). Thus, the magmatic intrusion distribution map (Figure 18) produced in the present study is considered reliable and provides insights on the subsurface geology and tectonic history of the study area. It shows that Early Cretaceous to Palaeogene HALIP magmatic bodies are much more widespread across the Mesozoic sedimentary successions of the Late Palaeozoic to Palaeogene Sverdrup Basin than implied by surface geological mapping.

6.2. Marginal sedimentary sub-basin mapping and its implications

The RTP-TMI anomaly data and their derivatives (Figures 5 – 9) were also used in identifying the actual location and extent of a distinct, major sedimentary sub-basin of the Canadian Arctic shelf, situated north of Meighen Island of the study area, called here the ‘Northeastern Canadian Arctic Marginal Basin’ (NECAMB) (Figure 18). From these magnetic anomaly maps (Figures 5 – 9), the boundaries of this NE-SW trending NECAMB can be clearly identified and the resulting map is shown in Figure 18. The NECAMB is bordered to the south by crustal basement highs associated with the Eurekan Orogeny, the Sverdrup Rim and onshore volcanic rocks of the Sverdrup Basin, to the north and northwest by the Alpha Ridge magmatic complex and to the northeast by volcanic rocks of Alpha Ridge – Ellesmere Island margin. The NECAMB totally lacks any signature of magmatic activity, a strong indication that it may be a product of an extensional tectonic event that post-dates the magmatism of the offshore Alpha Ridge. It has a total area of c. 54000 km² within the present study area, but generally appears run further southwestwards into the Beaufort Sea shelf region (Figures 1 and 2) and may be an prolongation of the deeper Beaufort-Mackenzie Basin. It is characterised by distinctive magnetic anomaly patterns comprising medium-wavelength, quasi-linear to curvilinear anomalies with moderately high to low amplitudes and low magnetic relief that are consistent with the occurrence of thick sedimentary successions (equivalently, greater depth to magnetic basement) and absence of intra-sedimentary magmatic intrusions (Figure 5). Its position nearly coincides with the shelf-slope area of the northeast CAM which exhibits bathymetric depths of c. 46 – 1852 m (Figure 1). The available published seismic velocity models across the region (Asudeh et al., 1989; Argyle and Forsyth, 1994; Forsyth et al., 1998; Funck et al., 2011) strongly support the presence of a major sedimentary sub-basin.

Although the previously published seismic refraction studies indicated the presence of a sedimentary basin in the region, they were not able to outline its areal extent. According to

Forsyth et al. (1998), the sedimentary succession is characterised by 5 – 10 km of lower velocity ($< \sim 5.2$ km/s) material of probable Late Cretaceous to Cenozoic age (i.e. the Arctic Terrace Wedge post-rift section). On the magnetic (RTP-TMI) anomaly map of the study area (Figure 5), the shelf edge seismically mapped by Forsyth et al. (1998) exhibits sub-linear to linear, broad medium- to long-wavelength magnetic anomalies with very high amplitudes and its position corresponds to a portion of the adjacent northwestern margin of the NECAMB characterised by the extensive volcanic and intrusive rocks of Alpha Ridge magmatic complex (Figure 18).

The potential field results, particularly the edge enhanced (derivative) magnetic anomaly maps (Figures 6 – 9), suggest that the NECAMB developed after the widespread magmatic activities associated with the emplacement of HALIP (manifested by Alpha Ridge) in the Early – Mid Cretaceous. It is accordingly interpreted to contain mainly Late Cretaceous to Recent sedimentary successions, in part presumably sourced from the Cenozoic Eurekan Orogen. NECAMB sediments are thickest in the central areas and thin abruptly adjacent to the Alpha Ridge magmatic complex (to the north, northwest and northeast areas), basement ridges and volcanic rocks (to the south and east areas), suggesting a fault-bounded basin that formed in an extensional or transtensional tectonic environment.

6.3. Tectonic implications of magmatic intrusion trends

The magmatic intrusion trends mapped across the Axel Heiberg and Ellesmere islands are not considered further here since published paleomagnetic studies reveal that counter-clockwise rotation of the Cretaceous magmatic rock bodies ranging from about 33° (Wynne et al., 1983) to 11° (Jackson and Halls, 1988) took place during several episodes of deformation that culminated in the Eurekan Orogeny. The present orientations may therefore not represent the original trends of these magmatic rocks at the time of their emplacement. However, the tectonic implications of their orientations in the Sverdrup Basin area, with the exception of the Eurekan Orogeny affected Axel Heiberg and Ellesmere islands, can be broadly discussed in the context of the influence of regional stress fields.

Structural studies in different parts of the world have shown that magmatic intrusions, especially dykes, are generally emplaced approximately normal to the direction of minimum principal compressive stress (e.g. Pollard, 1987; Marinoni, 2001 and references therein; Sinha

et al., 2011) and they are often interpreted as paleostress markers (Purucker and Whaler, 2015). If this is the case for the Sverdrup Basin area, including the northeasternmost parts of Axel Heiberg and Ellesmere islands relatively unaffected by the Eurekan Orogeny, then two minimum principal compressive stress directions, NE-SW and NW-SE, were present in the region during the emplacement of magmatic rock bodies inferred by the potential field analysis. Change in orientation of several elliptical saucer-shaped sills in the Ellef Ringnes Island, from north-northeast trends to north-northwest trends was recently interpreted by Evenchick et al. (2015) as indicative of a change in stress orientation between 126 and 121 Ma. In addition, two major Cretaceous magmatism events have been suggested by Jollimore (1986) for dyke swarm emplacement across the Queen Elizabeth Islands with the ENE trending dyke swarm predating the NW-N trending swarm. Further, according to Døssing et al. (2013a) the mid to late Hauterivian-early Barremian magmatic episode in the Queen Elizabeth Islands is likely manifested by the ENE to N-NW trending dyke swarm or only the major ENE-NE trending portion of this dyke swarm.

Accordingly, the emplacement of a majority of the NE-SW trending magmatic rock bodies inferred in the present study is likely to have occurred within a NW-SE regional minimum compressive stress field, possibly in the Hauterivian/Barremian – Aptian. That a similar stress field is implied by the dominant trends associated with the magmatic Alpha Ridge suggests that the majority of the magmatic rocks in the present study area may be related to the Alpha Ridge magmatism. The less prevalent NW-SE striking magmatic rock bodies may have been emplaced after the Aptian within a NE-SW minimum compressive stress orientation, following Evenchick et al.'s (2015) interpretation but the potential field patterns are not diagnostic in this respect and could also be sensing older basement trends that may be present. Based on the areal distribution of the present results, it is also not possible to speculate on the possibility of there being a radiating dyke swarm on the Queen Elizabeth Islands as proposed by Buchan and Ernst (2006).

7. Summary and Conclusions

This study was aimed at elucidating the regional subsurface geology and tectonics of the northeast CAM through detailed analysis and interpretation of potential field (gravity and magnetic) data constrained with available seismic refraction results and surface geological information. Five main magnetic domains have been recognised based on distinctive anomaly patterns/attributes and tectonic fabrics on the various magnetic anomaly maps combined with

their geology and geodynamic setting. Areal extents of the numerous magmatic and tectonic bodies (across the offshore Alpha Ridge and onshore Sverdrup Basin regions) as well as major sedimentary sub-basin (beneath the Canadian Arctic shelf region called here the ‘Northeastern Canadian Arctic Marginal Basin’; NECAMB) were delineated and mapped from the potential field data through the use of a variety of edge enhanced (derivative) methods. Positive magnetic and pseudogravity anomalies indicate high crustal magnetisation associated with the presence of extensive and voluminous, mafic magmatic bodies in the crust beneath Alpha Ridge region. The magmatic intrusion distribution map reveals that Early Cretaceous to Palaeogene magmatic bodies are far more prevalent across the Mesozoic sedimentary successions of the Sverdrup Basin than implied by surface geological mapping. The absence of magmatic intrusions in the well-imaged NECAMB suggests that its formation may have occurred in the Late Cretaceous – Cenozoic times after the cessation of the extensive magmatic activity associated with the Early – Mid Cretaceous Alpha Ridge igneous event. Additionally, most of magmatic rocks mapped in this study appear to have been emplaced during a major regional, NW-SE minimum compressive stress field that is more likely coeval with the Early Cretaceous (especially Hauterivian/Barremian – Aptian) HALIP magmatism.

Acknowledgements

We thank Dr Richard W. Saltus (U. S. Geological Survey, Colorado USA) for providing the new Circum-Arctic magnetic anomaly grid (CAMP-M) compilation dataset and the Geophysical Data Centre of the Geological Survey of Canada Ottawa for the gravity data used in this study. The first author (GKA) has been supported by the Nigerian Government scholarship through the academic staff training scheme of the Tertiary Education Trust Fund (TETFund) and the Management of the Nasarawa State University, Keffi Nigeria; hence, they are hereby gratefully acknowledged. We are grateful to the two anonymous reviewers, Dr Larry Lane (Guest Editor) and Prof. Rob Govers (Editor-in-Chief) for their constructive comments and suggestions which greatly improved the manuscript. This study is part of the Circum-Arctic Lithosphere Evolution (CALE) Project.

References

Aldana, M., Costanzo-Alvarez, V. And Diaz, M. 2003. Magnetic and mineralogical studies to characterise oil reservoirs in Venezuela. *Leading Edge*, Vol. 22, No. 6, p.526.

- Akima, H. 1970. A new method of interpolation and smooth curve fitting based on local procedures. *Journal of Association for Computing Machinery*, Vol. 17, No. 4, pp. 589-602.
- Anudu, G. K., Stephenson, R. A. and Macdonald, D. I. M. 2014. Using high-resolution aeromagnetic data to recognise and map intra-sedimentary volcanic rocks and geological structures across the Cretaceous middle Benue Trough Nigeria. *Journal of African Earth Sciences*, Vol. 99, No.2, pp.625-636.
- Argyle, M. and Forsyth, D. A. 1994. Interpretation of data and presentation of results from the Ice Island 1986 and 1990 seismic refraction experiments. *Geological Survey of Canada*, Open File No. 2973, 82p.
- Asudeh, I., Forsyth, D. A., Stephenson, R., Embry, A. F., Jackson, H. R. and White, D. 1989. Crustal structure of the Canadian polar margin: results of the 1985 seismic refraction survey. *Canadian Journal of Earth Sciences*, Vol. 26, pp. 853-866.
- Balkwill, H. R. 1978. Evolution of the Sverdrup Basin, Arctic Canada. *American Association of Petroleum Geologists (AAPG) Bulletin*, Vol. 62, No. 6, pp. 1004-1028.
- Balkwill, H. R. 1983. Geology of Amund Ringnes, Cornwall and Haig-Thomas Island, District of Franklin. *Geology Survey of Canada*, Memoir 390, 76p.
- BGR. 2014. BGR Polar Research. Volcanism in the Canadian Arctic and North Greenland related to the opening of the Arctic Ocean. http://www.bgr.bund.de/EN/Themen/Polarforschung/Projekte/Arktis_Projekte/vulkanismus_en.html (last accessed 20.06.14).
- Blakely, R. J. 1996. *Potential theory in gravity and magnetic applications*. Cambridge University Press, UK. 445p.
- Blakely, R. J. and Simpson, R. W. 1986. Approximating edges of source bodies from magnetic or gravity anomalies. *Geophysics*, Vol. 51, No. 7, pp. 1494-1498.
- Boutelier, J., Cruden, A., Brent, T. and Stephenson, R. 2011. Timing and mechanisms controlling evaporite diapirism on Ellef Ringnes Island, Canadian Arctic Archipelago. *Basin Research*, Vol. 23, No. 4, pp. 478-498.
- Briggs, I. C. 1974. Machine contouring using minimum curvature. *Geophysics*, Vol. 39, pp. 39-48.
- Bruvoll, V., Kristoffersen, Y., Coakley, B.J. and Hopper, J. 2010. Hemipelagic deposits on the Mendeleev and Alpha sub-marine ridges in the Arctic Ocean: acoustic stratigraphy, depositional environment and inter-ridge correlation calibrated by the ACEX results. *Marine Geophysical Research*, Vol. 31, pp.149-171. doi:10.1007/s11001-010-9094-9.
- Bruvoll, V., Kristoffersen, Y., Coakley, B., Hopper, J., Planke, S. and Kandilarov, A. 2012. The nature of the acoustic basement on Mendeleev and northwestern Alpha ridges, Arctic Ocean. *Tectonophysics*, Vols. 514-517, pp.123-145.
- Buchan, K. and Ernst, R. 2006. Giant dyke swarms and the reconstruction of the Canadian Arctic islands, Greenland, Svalbard and Franz Josef Land. In: Hanski, E., Mertanen, S., Rämö, T. (eds.), *Dyke Swarms: Time Markers of Crustal Evolution*. Taylor and Francis Group, London. pp. 27-48.
- Cordell, L. and Grauch, V. J. S. 1985. Mapping basement magnetization zones from aeromagnetic data in the San Juan Basin, New Mexico: In Hinze. W. J. (ed.). *The utility of regional gravity and magnetic anomaly maps*: SEG, pp. 181-197.

Cooper, G. R. J. and Cowan, D. R. 2004. Filtering using variable order vertical derivatives. *Computers and Geosciences*, Vol. 30, pp. 455-459.

Costanzo-Alvarez, V., Aldana, M., Aristeguieta, O., Marcano, M. C. and Aconcha, E. 2000. Study of magnetic contrasts in the Guafita oil field (south-western Venezuela). *Phy. Chem. Earth Part A: Solid Earth Geodesy*, Vol. 25, No. 5, pp. 437-445.

Dobrin, M.B. and Savit, C. H. 1988. *Introduction to Geophysical Prospecting*, 4th edition, McGraw-Hill, New York. 867p.

Døssing, A., Jackson, H., Matzka, J., Einarsson, I., Rasmussen, T., Olesen, A.V. and Brozena, J. 2013a. On the origin of the Amerasia Basin and the High Arctic Large Igneous Province – results of new aeromagnetic data. *Earth and Planetary Science Letters*, Vol. 363, pp. 219-230.

Døssing, A., Hopper, J. R., Olesen, A. V., Rasmussen, T. M. and Halpenny, J. 2013b. New aero-gravity results from the Arctic Ocean: Linking the latest Cretaceous-early Cenozoic plate kinematics of the North Atlantic and Arctic Ocean, *Geochem. Geophys. Geosyst.*, Vol. 14, No. 10, pp. 4044–4065.

Embry, A. and Osadetz, K. 1988. Stratigraphy and tectonic significance of Cretaceous volcanism in the Queen Elizabeth Islands, Canadian Arctic Archipelago. *Canadian Journal of Earth Sciences*, Vol. 25, No. 8, pp.1209-1219.

Embry, A. F. 1990. Geological and geophysical evidence in support of the hypothesis of anticlockwise rotation of northern Alaska. *Marine Geology*, Vol. 93, pp. 317-329.

Embry, A. F. 1991. Mesozoic history of the Arctic Islands: In: Trettin, H. P. (ed.), *Geology of the Innuitian orogen and Arctic platform of Canada and Greenland*. Geology Survey of Canada, Geology of Canada, No. 3, pp.371- 433.

Embry, A. F. and Dixon, J. 1990. The breakup unconformity of the Amerasia Basin, Arctic Ocean: Evidence from Arctic Canada. *Geological Society of America Bulletin*, Vol. 102, pp. 1526-1534.

Embry, A. F. and Beauchamp, B. 2008. Sverdrup Basin. In: Miall, A. D. (ed.), *The Sedimentary Basins of the United States and Canada*, Vol. 5 (Sedimentary basin of the world), Elsevier, Amsterdam. pp. 451-471.

Estrada, S. and Henjes-Kunst, F. 2004. Volcanism in the Canadian High Arctic related to the opening of the Arctic Ocean. *Zeitschrift der Deutschen Geologischen Gesellschaft*, Vol. 154, No. 4, pp. 579-603.

Estrada, S., Piepjohn, K., Henjes-Kunst, F. and von Gosen, W. 2006. Geology, magmatism and structural evolution of the Yelverton Bay area, Northern Ellesmere Island, Arctic Canada. *Polarforschung*, Vol. 73, No. 2/3, pp. 59-75.

Evenchick, C. A., Davis, W. J., Bedard, J. H., Hayward, N. and Friedman, R. M. 2015. Evidence for protracted High Arctic large igneous province magmatism in the central Sverdrup Basin from stratigraphy, geochronology and paleodepths of saucer-shaped sills. *GSA Bulletin*, Vol. 127, No. 9/10, pp. 1366-1390.

Forsyth, D. A., Mair, J. A. and Fraser, I. 1979. Crustal structure of the central Sverdrup Basin. *Canadian Journal of Earth Sciences*, Vol. 16, No. 8, pp. 1581-1598.

Forsyth, D.A., Asudeh, I., Green, A.G. and Jackson, H.R. 1986a. Crustal structure of the northern Alpha Ridge beneath the Arctic Ocean. *Nature*, Vol. 322, pp. 349-352.

Forsyth, D.A., Morel-a-l'Huissier, P., Asudeh, I., Green, A.G., Johnson, G.L. and Kaminuma, K., 1986b. Alpha Ridge and Iceland; products of the same plume? *Journal of Geodynamics*, Vol. 6, pp. 197-214.

Forsyth, D.A., Broome, J., Embry, A.F. and Halpenny, J.F. 1990. Features of the Canadian polar margin. In: J.R. Weber, D.A. Forsyth, A.F. Embry and S.M. Blasco (Eds.), *Arctic Geoscience. Marine Geology*, Vol. 93, pp. 147-177.

Forsyth, D.A., Asudeh, I., White, D., Jackson, R., Stephenson, R.A., Embry, A.F. and Argyle, M. 1998. Sedimentary basins and basement highs beneath the Polar Shelf north of Axel Heiberg and Meighen Islands. *Bulletin of Canadian Petroleum Geology*, Vol. 46, No. 1, pp. 12-29.

Funck, T., Jackson, R. H. and Shimeld, J. 2011. The crustal structure of the Alpha Ridge at the transition to the Canadian Polar Margin: Results from a seismic refraction experiment. *Journal of Geophysical Research*, Vol. 116, B12101, 26p.doi: 10.1029/2011JB008411.

Gaina, C., Werner, S. C., Saltus, R., Maus, S. and the CAMP-GM Group. 2011. Circum-Arctic mapping project: new magnetic and gravity anomaly maps of the Arctic. Spencer, A. M., Embry, A. F., Gautier, D. L., Stoupakova, A. V. and Sørensen, K. (eds.) *Arctic Petroleum Geology. Geological Society of London, Memoirs*, 35, pp. 39-48.

Geosoft Inc. 2008. Oasis montaj MAPS v7.0: Getting started with the Oasis montaj help topics. Geosoft Inc., Canada. Contained in the Help menu of the Oasis montajv7.0 software.

Geosoft Inc. 2011. MAGMAP Filtering. Technical Documentation. Tutorial. Geosoft Inc., Canada. www.geosoft.com/support/downloads/technical-documentation (last accessed 20.03.12).

Geosoft Inc. 2012. Oasis montaj gridding. 20p. www.geosoft.com/resources/goto/oasis-montaj-gridding (last accessed 31.05.13).

GETECH Group Plc. 2007. Advanced processing and interpretation of gravity and magnetic data. GETECH (Geophysical Exploration Technology) Group Plc. Kitson House Elmete Hall Leeds, UK. 22p.

Grantz, A., Hart, P.E. and Childers, V.A. 2011. Geology and tectonic development of the Amerasia and Canada Basins, Arctic Ocean. In: Spencer, A. M., Embry, A. F., Gautier, D. L., Stoupakova, A. V. and Sørensen, K. (eds.), *Arctic Petroleum Geology. Geological Society, London, Memoirs*, Vol. 35, pp. 771-799.

Gottlieb, E. S., Meisling, K. E., Miller, E. L. and "Gil" Mull, C. G. 2014. Closing the Canada Basin: Detrital zircon geochronology relationships between the North Slope of Arctic Alaska and the Franklinian mobile belt of Arctic Canada. *Geosphere*, Vol. 10, No. 6, pp. 1-19.

Harrison, J. C., St-Onge, M. R., Petrov, O.V, Strelnikov, S. I, Lopatin, B. G, Wilson, F. H, Tella, S., Paul, D., Lynds, T., Shokalsky, S. P, Hulst, C. K, Bergman, S., Jepsen, H. F. and Solli, A. 2011. Geological map of the Arctic; Geological Survey of Canada, Map 2159A, scale 1: 5 000 000.

Harry, D. L. 2008. Geodynamic Constraints on Opening of the Gulf of Mexico and the Nature of the Crust. *Geological Society of America Abstracts with Programs*, Vol. 40, No. 6, p.445.

Hinze, W.J., Von Frese, R. R. B. and Saad, A. H. 2013. Gravity and Magnetic Exploration. Principles, Practices and Applications. Cambridge University Press, New York. 512p.

- IGC. 1996. Glossary of gravity and magnetic terms: A guide to the language of geophysical interpretation. Integrated Geophysics Corporation (IGC) Houston, Texas. http://www.igcworld.com/gm_glos.html (last accessed 20.02.15).
- Jackson, H. R. 1985. Seismic reflection results from CESAR. In: Jackson, H.R., Mudie, P., Blasco, S.M. (Eds.), Initial geological Report on CESAR — the Canadian Expedition to Study the Alpha Ridge, Arctic Ocean: Geol. Survey of Canada, Paper, 84–22, pp. 19–23.
- Jackson, K.C. and Halls, H.C. 1988. Tectonic implications of paleomagnetic data from sills and dykes in the Sverdrup Basin, Canadian Arctic. *Tectonics*, Vol.7, pp. 463-481.
- Jacoby, W. and Smilde, P. L. 2009. Gravity Interpretation: Fundamentals and application of gravity inversion and geological interpretation. Springer-Verlag Berlin Heidelberg. 387p.
- Jakobsson, M., et al. 2012. The International Bathymetric Chart of the Arctic Ocean (IBCAO) Version 3.0. *Geophysical Research Letters*, Vol. 39, L12609, doi:10.1029/2012GL052219.
- Jokat, W. 2003. Seismic investigations along the western sector of Alpha Ridge, Central Arctic Ocean. *Geophysical Journal International*, Vol. 152, pp. 185-201.
- Jokat, W., Stein, R., Rajor, E., Schewe, I. and the Shipboard Scientific Party. 1999. Expedition gives fresh view of Central Arctic geology. *EOS, Transactions American Geophysical Union*, Vol. 80, No. 40, pp. 465-473.
- Jollimore, W. 1986. Analyses of dyke swarms within the Sverdrup Basin, Queen Elizabeth Islands, District of Franklin. Unpublished B.Sc. Thesis, Dalhousie University, Halifax, Nova Scotia.
- Kenyon, S., Forsberg, R. and Coakley, B. 2008. New gravity field for the Arctic. *EOS*, Vol. 89, No. 32, pp. 1-2.
- Lane, S. L., Gehrels, G. E. and Layer, P. W. 2016. Provenance and palaeogeography of the Neruokpuk Formation, northwest Laurentia: An integrated synthesis. *Geological Society of America (GSA) Bulletin*, Vol. 128; No. 1/2, pp. 239-257.
- Laxon, S. and McAdoo, D. 1994. Arctic Ocean gravity field derived from ERS-1 satellite altimetry. *Science*, Vol. 265, No. 5172, pp. 621-624.
- Macleod, I. N., Jones, K. and Dai, T. F. 1993. 3-D Analytic signal in the interpretation of total magnetic field data at low magnetic latitudes. *Exploration Geophysics*, Vol. 24, pp. 679-688.
- Marinoni, L. B. 2001. Crustal extension from exposed sheet intrusions: Review and method proposal. *Journal of Volcanology and Geothermal Research*, Vol. 107, pp. 27-46.
- Maus, S., Sazonova, T., Hemant, K., Fairhead, J. D. and Ravat, D. 2007. National Geophysical Data Centre candidate for the World Digital Magnetic Anomaly Map. *Geochemistry Geophysics Geosystems*, Vol. 8, No. 6, Q06017, doi:10.1029/2007GC001643
- Maus, S. et al. 2009. EMAG2: A 2-arc-minute resolution Earth Magnetic Anomaly Grid compiled from satellite, airborne, and marine magnetic measurements, *Geochemistry Geophysics Geosystems*, Vol. 10, No. 8, Q08005, doi:10.1029/2009GC002471.
- Miller, H. G. and Singh, V. 1994. Potential field tilt – a new concept for location of potential field sources. *Journal of Applied Geophysics*, Vol. 32, pp. 213-217.

- Milligan, P. R. and Gunn, P. J. 1997. Enhancement and presentation of airborne geophysical data. *AGSO Journal of Australian Geology and Geophysics*, Vol. 17, No. 2, pp. 63-75.
- Moore, T.E., Wallace, W., Bird, K., Karl, S., Mull, C.G. and Dillon, J. 1994. Geology of Northern Alaska. *The geology of Alaska: Boulder, Colorado, Geological Society of America, Geology of North America*, 1, 49-140.
- Mühe, R. and Jokat, W. 1999. Recovery of volcanic rocks from the Alpha Ridge, Arctic Ocean: preliminary results. *EOS, Trans. AGU*, 80. F1000, San Francisco.
- NAMAG (NORTH AMERICAN MAGNETIC ANOMALY GROUP). 2002. Magnetic Anomaly Map of North America. US Geological Survey Special Map, scale 1:10 000 000.
- NOAA/NGDC. 2010. World magnetic model – epoch 2010: Main field inclination. National Oceanic and Atmospheric Administration (NOAA)/National Geophysical Data Centre (NGDC), Colorado USA. <http://ngdc.noaa.gov/geomag/WMM/> (last accessed 04.07.14)
- Oakey, G. N. and Stephenson, R. 2008. Crustal structure of the Innuitian region of Arctic Canada and Greenland from gravity modelling: implications for the Palaeogene Eurekan orogen. *Geophysical Journal International*, Vol. 173, pp. 1039-1063.
- Oakey, G. N., Damaske, D. and Nelson, B. 2012. Geology and volcanism along the Canadian Arctic margin: New constraints from aeromagnetic mapping. *International Polar Year 2012, Montreal. Abstracts volume*.
- Okulitch, A V. 1991. Geology of the Canadian Arctic Archipelago, Northwest Territories and North Greenland. Geological Survey of Canada, "A" Series Map 1715A, 1991; 1 sheet, doi:10.4095/213121.
- Parasnis, D.S. 1986. *Principles of Applied Geophysics*. 4th edition. Chapman and Hall, New York. 402p.
- Phillips, J. D. 1998. Processing and interpretation of aeromagnetic data from Santa Cruz Basin-Patahonia mountains area, south-central Arizona. US Geological Survey Open-File Report 02-98.
- Piskarev, A. L. 2004. The basement structure of the Eurasian Basin and central ridges in the Arctic Ocean. *Geotectonics*, Vol. 38, pp. 443-458.
- Pollard, D. D. 1987. Elementary fracture mechanics applied to the structural interpretation of dykes. In: Halls, H.C., Fahrig, W.F. (Eds.), *Mafic Dyke Swarms*. Geol. Assoc. Canada Spec. Pap. 34, pp. 5–24.
- Purucker, M. E. and Whaler, K. A. 2015. Crustal magnetism. In: Schubert, G. (ed.), *Treatise on Geophysics* (2nd Edition). Elsevier, Oxford UK. pp. 187-211.
- Richard, B., John, T. and Brad, S. 2013. Cretaceous magmatism in the High Canadian Arctic: Implications for the nature and age of Alpha Ridge. *Geophysical Research Abstracts*, Vol. 15, EGU2013-11429-1.
- Ricketts, B., Osadetz, K.G. and Embry, A. F. 1985. Volcanic style in the Strand Fiord Formation (Upper Cretaceous), Axel Heiberg Island, Canadian Arctic Archipelago. *Polar Research*, Vol. 3, No. 1, pp. 107-122.
- Reeves, C. 2005. *Aeromagnetic Surveys: Principles, practice and interpretation*. Geosoft. 68p.
- Roest, W. R., Verhoef, J. and Pilkington, M. 1992. Magnetic interpretation using the 3-D analytic signal. *Geophysics*, Vol. 57, pp. 116-125.

Saltus, R.W., Meyer, J.F., Barnes, D.F., and Morin, R.L. 1997. Tectono-geophysical domains of interior Alaska as interpreted from new gravity and aeromagnetic data compilations. In Dumoulin, J.A. and Gray, J.E. (eds.), *Geologic studies in Alaska by the U.S. Geological Survey, 1995: U.S. Geological Survey Professional Paper 1574*, pp. 157-171.

Saltus, R. W., Miller, E. L., Gaina, C. and Brown, P. J. 2011. Regional magnetic domains of the Circum-Arctic: a framework for geodynamic interpretation. In: Spencer, A. M., Embry, A. F., Gautier, D. L., Stoupakova, A. V. and Sørensen, K. (eds.) *Arctic Petroleum Geology*. Geological Society of London, *Memoirs*, 35, pp. 49-60.

Sheriff, R.E. 2002. *Encyclopedic Dictionary of Applied Geophysics*, 4th edition. 13 Geophysical Reference Series. Society of Exploration Geophysicists, Tulsa USA, 429p.

Sinha, D. K., Jain, S. K. and Naganath, K. P. 2011. Tectonic significance and age of doleritic sill near Bandhalimal in the Singhora Protobasin of Chhattisgarh Basin, central India. In: Srivastava, R. K. (ed.), *Dyke swarms: Keys for geodynamic interpretation*. Springer-Verlag Berlin Heidelberg. pp. 167-187.

Sobczak, L.W. 1975. Gravity and deep structure of the continental margin of Banks Island and Mackenzie Delta. *Canadian Journal of Earth Sciences*, Vol. 12, pp. 378-394.

Sobczak, L.W., Mayr, U. and Sweeney, J.F. 1986. Crustal section across the polar continent ocean transition in Canada. *Canadian Journal of Earth Sciences*, Vol. 23, pp. 608-621.

Stephenson, R. A., Embry, A. F., Nakiboglu, S. M. and Hastaoglu, M. A. 1987. Rift-initiated Permian to Early Cretaceous subsidence of the Sverdrup Basin. In: Beaumont, C. and Tankard, A. J. (eds.), *Sedimentary Basins and Basin-forming Mechanisms*. Canadian Society of Petroleum Geologists, *Memoir* 12, pp. 213-231.

Stephenson, R. A. and Ricketts, B. D. 1990. Bouguer gravity anomalies and speculations on the regional structure of the Eurekan Orogen, Arctic Canada. In: Weber, J. R., Forsyth, D. A., Embry, A. F. And Blasco, S. M. (eds.), *Arctic Geoscience. Marine Geology*, Vol. 93, pp. 401-420.

Stephenson, R. A., Ricketts, B. D., Cloetingh, S. A. and Beekman, F. 1990. Lithosphere folds in the Eurekan Orogen, Arctic Canada? *Geology*, Vol. 18, pp.603-606.

Stephenson, R. A. and Smolyaninova, E. I. 1999. Neotectonics and seismicity in the southeastern Beaufort Sea polar continental margin of northwestern Canada. *Journal of Geodynamics*, Vol. 27, pp. 175-190.

Stephenson, R. A., Van Berkel, J. T. and Cloetingh, S. A. P. L. 1992. Relation between salt diapirism and the tectonic history of the Sverdrup Basin Arctic Canada. *Canadian Journal of Earth Sciences*, Vol. 29, pp. 2695-2705.

Stephenson, R. A., Coflin, K. C., Lane, L. S. and Dietrich, J. R. 1994. Crustal structure and tectonics of the southeastern Beaufort Sea continental margin. *Tectonics*, Vol. 13, No. 2, pp. 389-400.

Stott, D. F. 1969. Ellef Ringnes Island Canadian Arctic Archipelago. Geological Survey of Canada, Paper 68-116.

Tailleur, I. L. 1973. Probable rift origin of Canada Basin, Arctic Ocean. In: Pitcher, M. (ed.), *Arctic Geology*. American Association of Petroleum Geologists *Memoir*, Vol. 19, pp. 526-535.

Telford, W. M., Geldart, L. P. and Sheriff, R. E. 1998. *Applied Geophysics*, 2nd edition, Cambridge University Press, USA.770p.

- Trettin, H. P. 1989. The Arctic Islands. In: Bally, A. W. and Palmer, A. R. (eds.), *The Geology of the North America – An Overview. The Decade of North American Geology*, Boulder, Colorado, Vol. A, pp. 349-370.
- Trettin, H. P. ed. 1991. *Geology of the Inuitian orogen and Arctic platform of Canada and Greenland*. Geology Survey of Canada, Geology of Canada, No. 3, 569p.
- Trettin, H. P. and Parrish, R. 1987. Late Cretaceous bimodal magmatism, northern Ellesmere Island: isotope age and origin. *Canadian Journal of Earth Sciences*, Vol. 24, pp. 257-265.
- Van Wagoner, N. A. and Robinson, P. T. 1985. Petrology and geochemistry of a CESAR bedrock sample; implications for the origin of the Alpha Ridge. *Geological Survey of Canada, Paper 84-22*, 47-58.
- Verduzco, B., Fairhead, J. D., Green, C. M. and Mackenzie, C. 2004. New insights into magnetic derivatives for structural mapping. *The Leading Edge*, Vol. 23, pp.116-119.
- Verhoef, J., Roest, W. R., Macnab, R. and Arkani, H. J. 1996. *Magnetic anomalies of the Arctic and North Atlantic Oceans and adjacent areas, CD Compilation*. Geological Survey of Canada, Ottawa.
- Vogt, P. R., Jung, W-Y. and Brozena, J. 1998. Arctic margin gravity highs: Deeper meaning for sediment depocenters? *Marine Geophysical Researches*, Vol. 20, pp. 459-477.
- Weber, J. R. 1990. The structures of the Alpha Ridge, Arctic Ocean and Iceland-Faeroe Ridge, North Atlantic; comparisons and implications for the evolution of the Canada Basin. *Marine Geology*, Vol. 93, pp. 43-68.
- Wijins, C., Perez, C. and Kowalezyk, P. 2005. Theta map: Edge detection in magnetic data. *Geophysics*, Vol. 70, pp. L39-L43.
- Williamson, M.-C., Smyth, H. R., Peterson, R. C. and Lavoie, D. 2011. Comparative geological studies of volcanic terrain on Mars: Examples from the Isachsen Formation, Axel Heiberg Island, Canadian High Arctic. In: Garry, W.B. and Bleacher, J.E. (eds.), *Analogues for Planetary Exploration*. Geological Society of America Special Paper 483, Pp. 249-261, doi:10.1130/2011.2483(16).
- Wynne, P. J., Irving, E. and Osadetz, K. G. 1983. Paleomagnetism of Cretaceous volcanic rocks of the Sverdrup Basin – magnetostratigraphy, paleolatitudes and rotations. *Canadian Journal of Earth Sciences*, Vol. 25, pp. 1220-1239.
- Zhetan, L., Ruixiang, Z. And Liansheng, H. 1980. Tectonics and deposits of the Cenozoic Era in the South China Sea. *Energy*, Vol. 6, No. 11, pp. 1093-1098.

FIGURES AND CAPTIONS

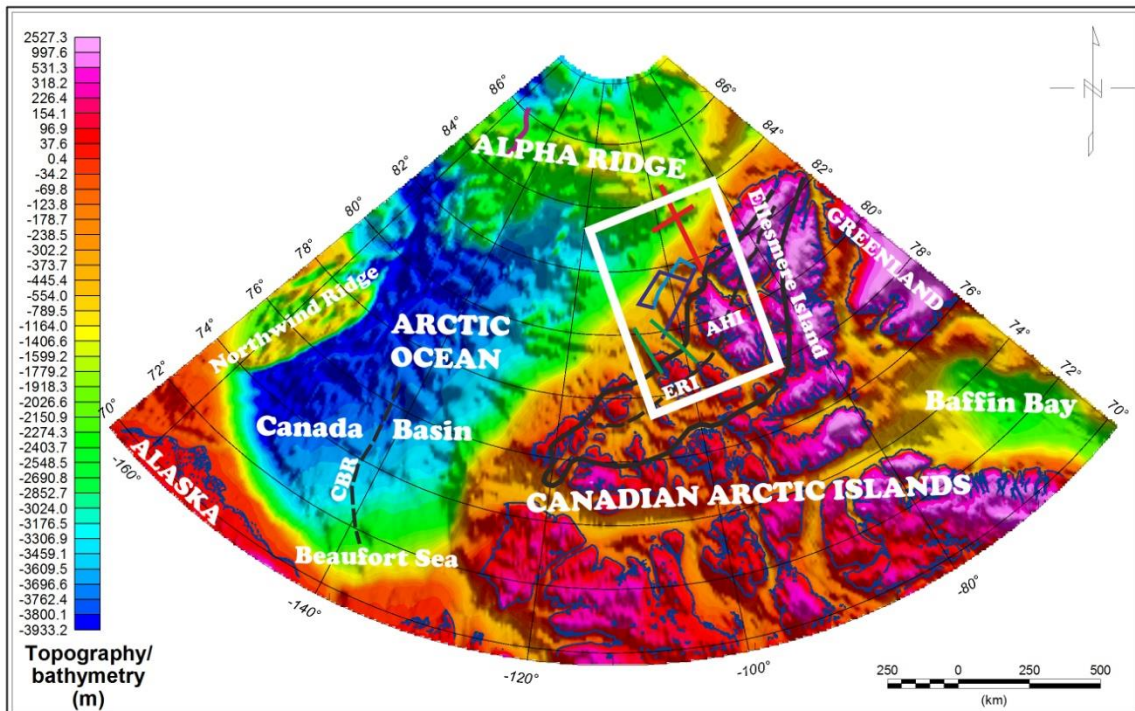


Figure 1. Relief bathymetry and topography map of the Canadian Arctic region showing the major geological and tectonic features of the region. Colour shaded and histogram equalised image illuminated from the north with colour variations depicting bathymetric depths and land elevations. Data grids were downloaded from the IBCAO Version 3.0 gridded bathymetry/topography dataset compilations (Jakobsson et al., 2012; available at <http://www.ngdc.noaa.gov/mgg/bathymetry/arctic/ibcaoversion3.html>) and later re-projected and geo-referenced. Location of the study area is marked with a white rectangular box. The Sverdrup Basin outline (bold black lines) is from Stephenson et al. (1987). Position of the extinct seafloor spreading ridge of Canada Basin (CBR; black solid line) is based on coincident regional, narrow linear negative Free-Air gravity anomalies (narrow linear gravity lows; Laxon and McAdoo, 1994; Grantz et al., 2011; Figure 2a). Red lines mark the ARTA 2008 seismic refraction profiles (Funck et al., 2011); purple line Healy 2005 seismic reflection profile (Bruvoll et al., 2012); green lines Ice Island 1990 seismic refraction profiles (Argyle and Forsyth, 1994); blue lines Ice Island 1986 seismic refraction profiles (Forsyth et al., 1998) and sky blue lines Ice Island 1985 seismic refraction profiles (Asudeh et al., 1989). AHI = Axel Heiberg Island; ERI = Ellef Ringnes Island. Map projection and datum on all figures are Universal Polar Stereographic North and World Geodetic System (WGS84).

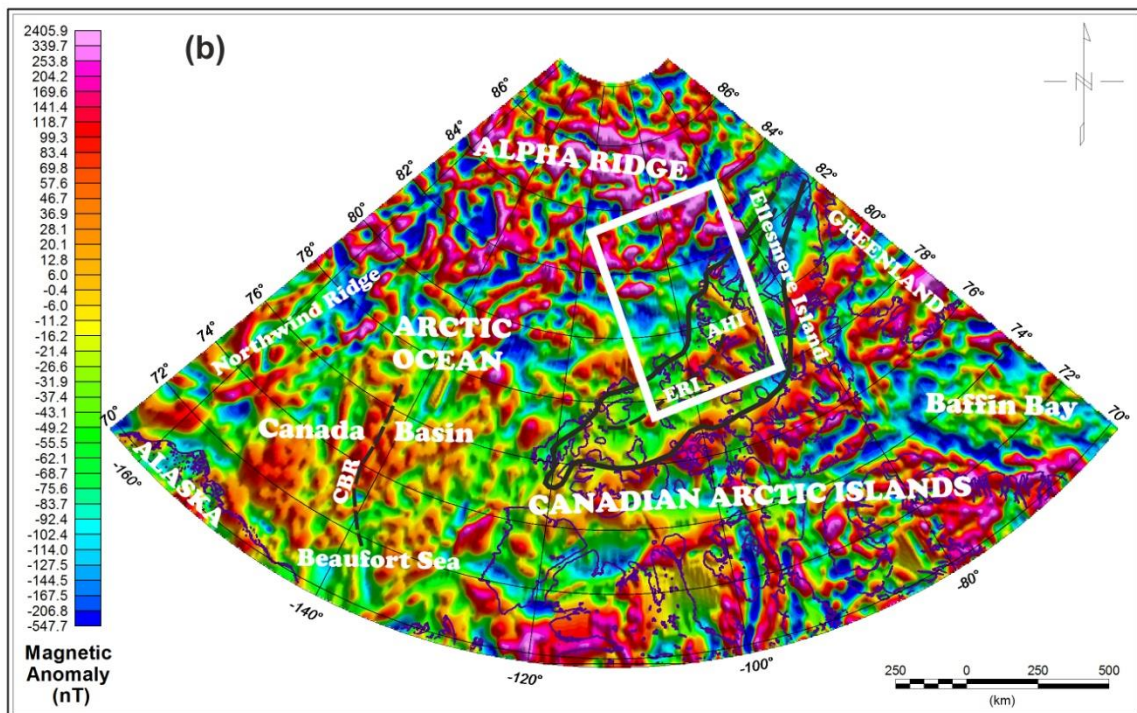
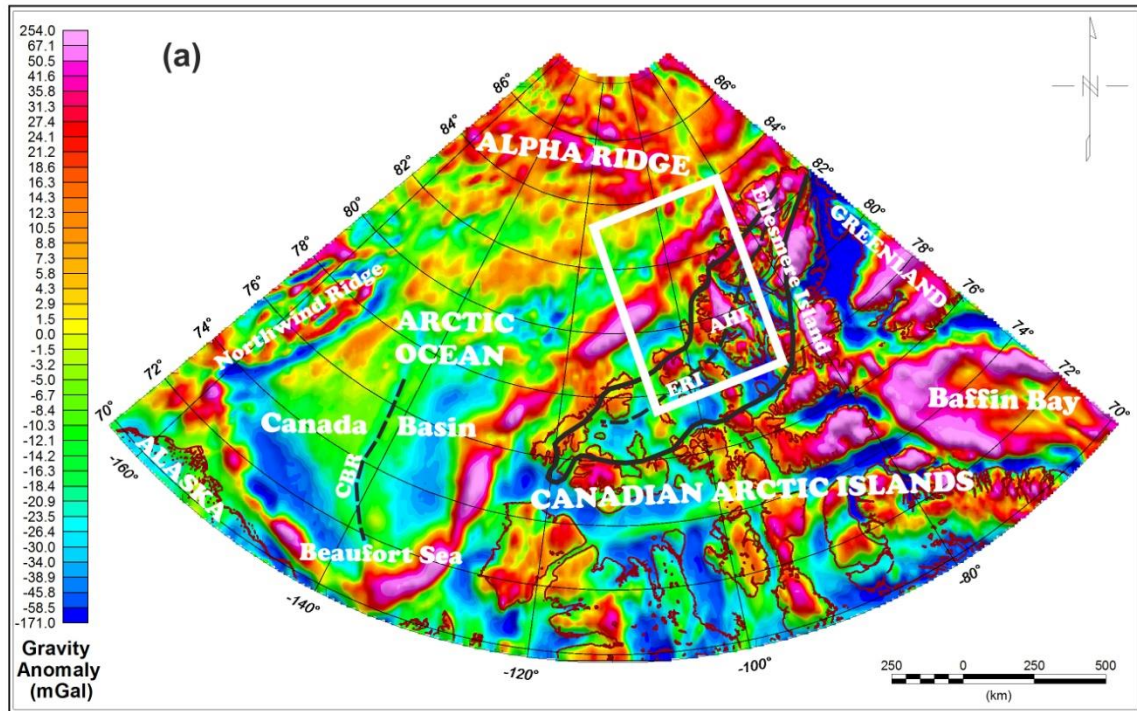


Figure 2. Potential field anomaly maps of the Canadian Arctic region. (a) Gravity anomaly map and (b) Magnetic anomaly map. The gravity data grid was downloaded from the Arctic Gravity Project (ArcGP; <http://earth-info.nga.mil/GandG/wgs84/agp/index.html>), an international compilation of public domain Free-Air and Bouguer anomaly grids for the Circum-Arctic region north of 64° N (Kenyon et al., 2008), while the magnetic data grid was extracted from the new Circum-Arctic magnetic anomaly grid (CAMP-M) dataset compilations (Gaina et al., 2011; Saltus et al., 2011). Respective grids were later re-projected and geo-referenced. Both maps also show the major geological and tectonic features across the region. Location of the study area is marked with white rectangular box. The Sverdrup Basin outline (bold black lines) is from Stephenson et al. (1987). CBR is the linear gravity anomaly low corresponding to the widely speculated extinct seafloor spreading ridge of Canada Basin (Laxon and McAdoo, 1994; Grantz et al., 2011); its position on the magnetic anomaly map is marked by solid black line. AHI = Axel Heiberg Island; ERI = Ellef Ringnes Island.

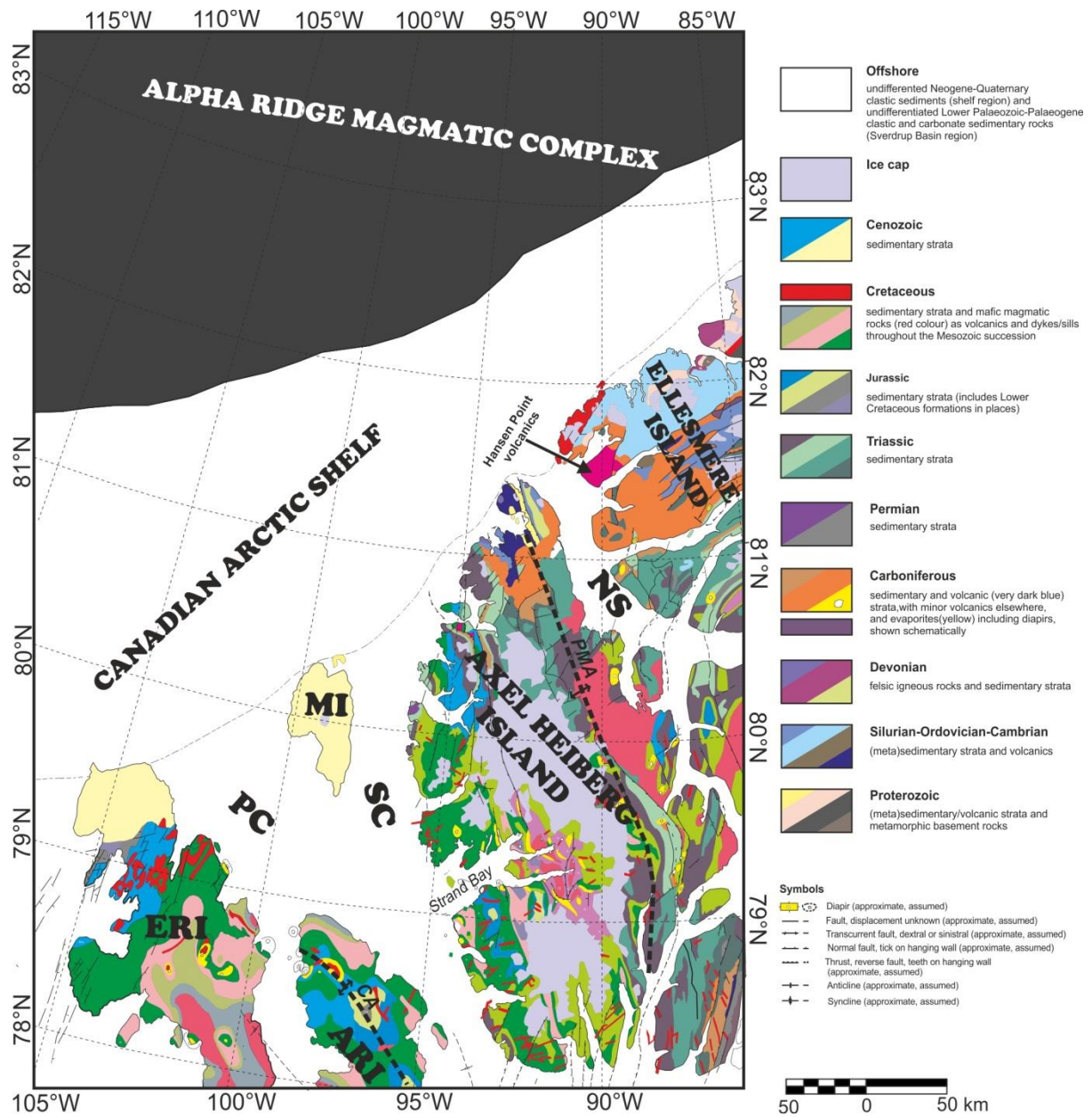


Figure 3. Detailed geological map of the study area. The major part of the map is extracted and modified from Okulitch (1991), with added information from Harrison et al. (2011). The positions of the Princess Margaret Arch (PMA) and Cornwall Arch (CA) are from Stephenson and Ricketts (1990) and Forsyth et al. (1998). ARI = Amund Ringnes Island; ERI = Ellef Ringnes Island; MI = Meighen Island; NS = Nansen Sound; SC = Sverdrup Channel; PC = Peary Channel.

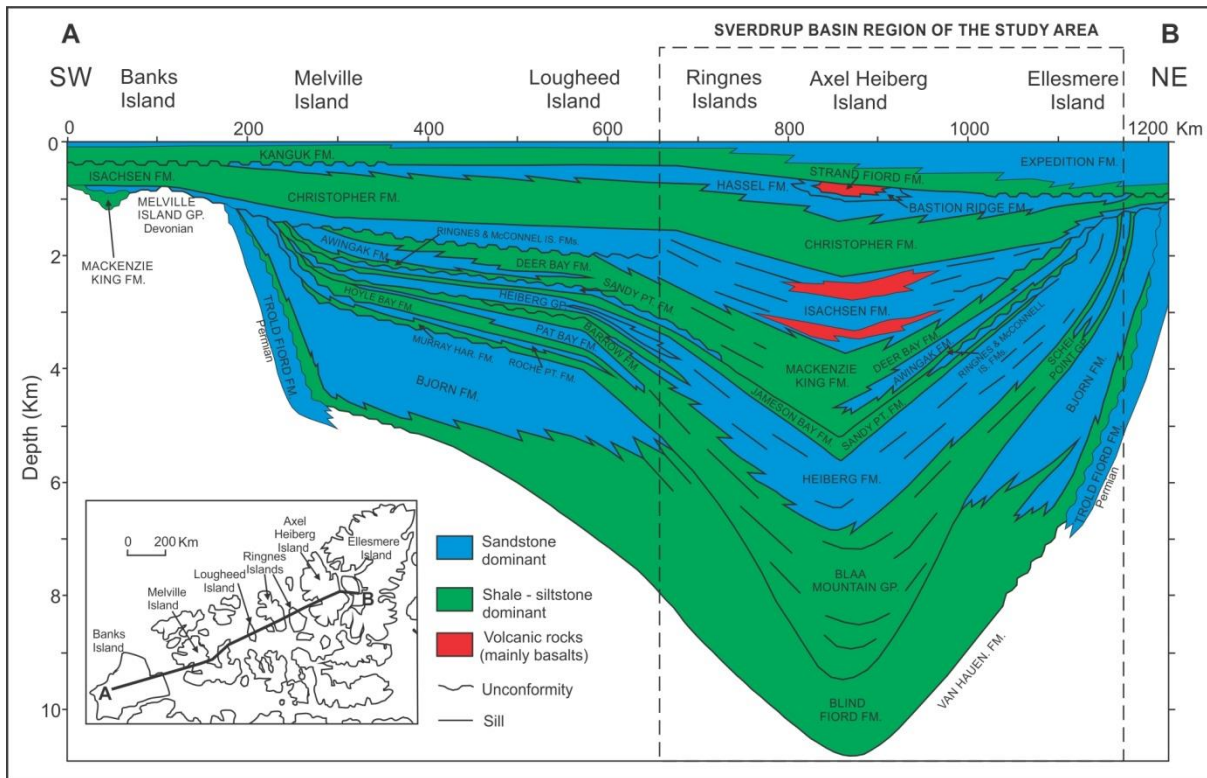


Figure 4. Schematic stratigraphic cross-section across the Banks Island and Sverdrup Basin (modified from Embry, 1991; Williamson et al., 2011). Positions of the volcanic rocks (mainly basalts) within the Isachen and Strand Fiord formations are shown in red, whereas the sills which occur in most Mesozoic sedimentary successions are shown with solid black lines. The location of the study area is marked with a dashed black rectangular box.

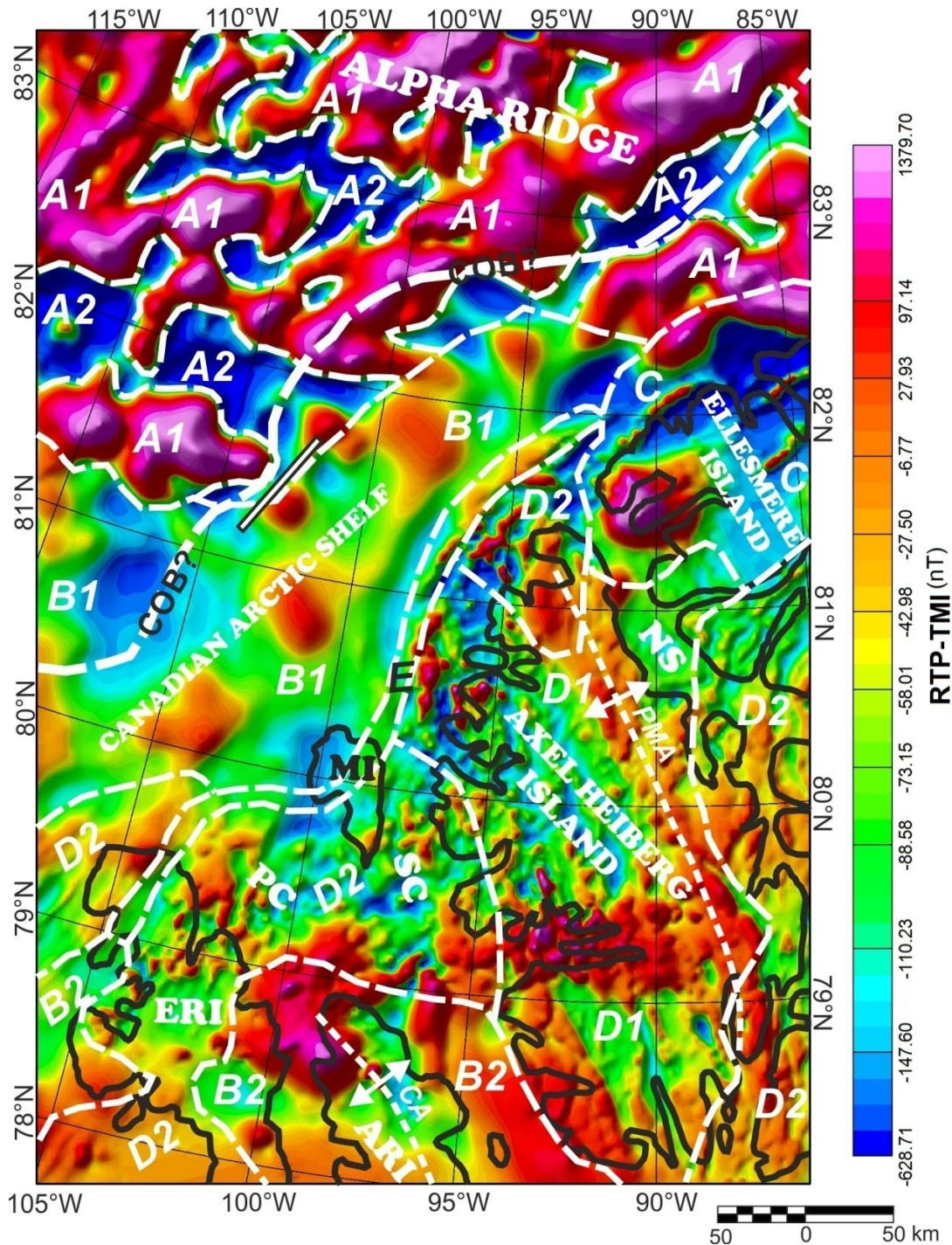


Figure 5. Reduced to Pole total magnetic intensity (RTP-TMI) anomaly map of the study area. Superimposed on it are the delineated five main magnetic domains: A, B, C, D and E which are further subdivided into sub-domains A1, A2, B1, B2, D1 and D2. These magnetic domains are shown in all edge enhanced (derivative) magnetic anomaly maps (Figures 6 - 9) and also comprehensively discussed in Section 5.1 of this paper. Also note the conspicuous absence of high amplitude, short wavelength magnetic anomalies within the Canadian Arctic Shelf region (sub-domain B1). The positions of the Princess Margaret Arch (PMA) and Cornwall Arch (CA) on all figures are from Stephenson and Ricketts (1990) and Forsyth et al. (1998). The continent-ocean boundary (COB?) shown as dashed white line on all the figures is after Oakey and Stephenson (2008) and coincides with the regional, well-defined maxima on the total horizontal derivative (THD) gravity anomaly map (Figure 17). Position of the “shelf edge high” seismically mapped by Forsyth et al. (1998) is marked as a thick white line with black outline. Note that on all figures: ARI = Amund Ringnes Island; ERI = Ellef Ringnes Island; MI = Meighen Island; NS = Nansen Sound; SC = Sverdrup Channel; PC = Peary Channel.

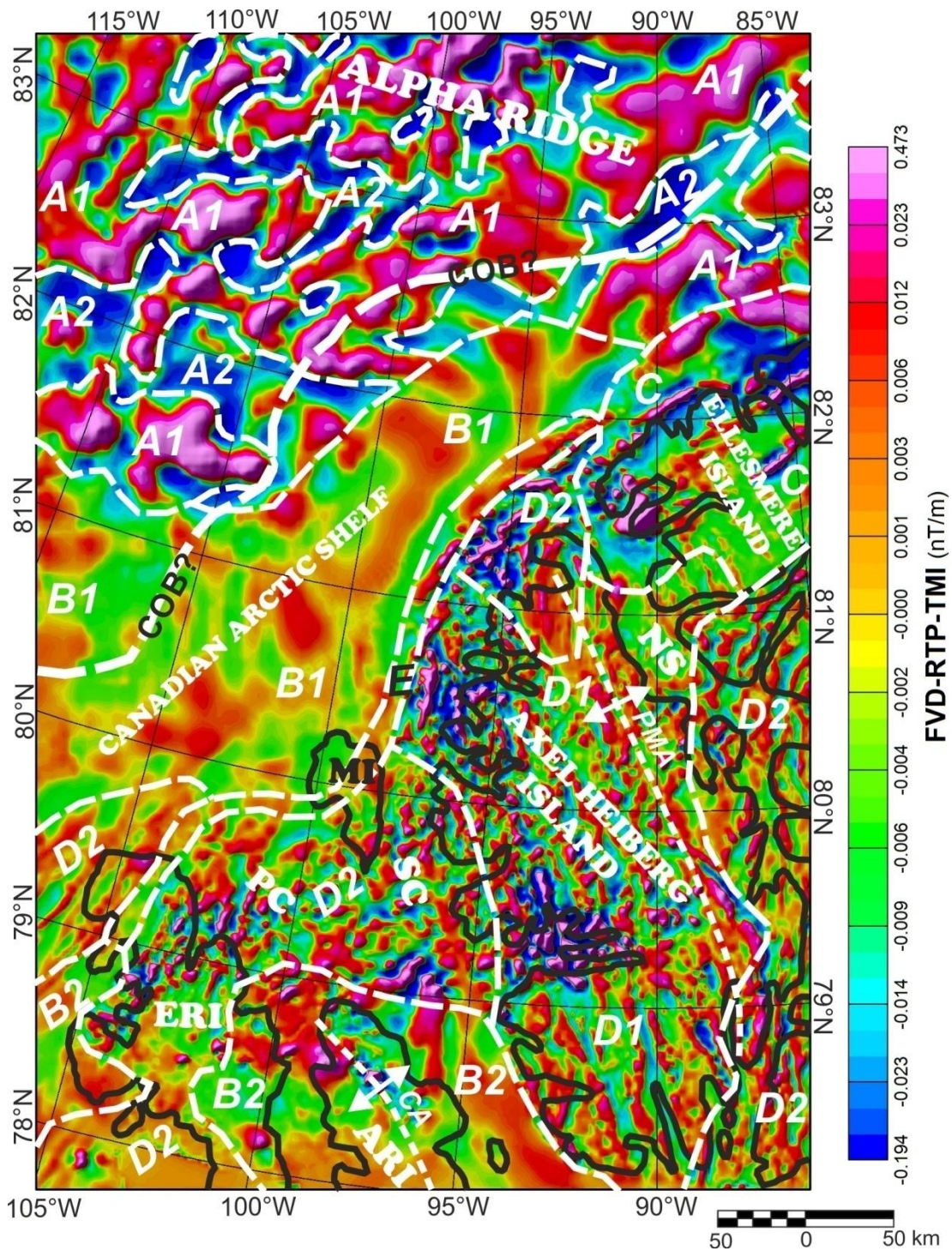


Figure 6. First vertical derivative of Reduced to Pole total magnetic intensity (FVD-RTP-TMI) anomaly map of the study area. The edges of high amplitude, short wavelength magnetic anomalies associated with the underlying magmatic rock bodies and other tectonic features are greatly enhanced, delineated and mapped on the figure.

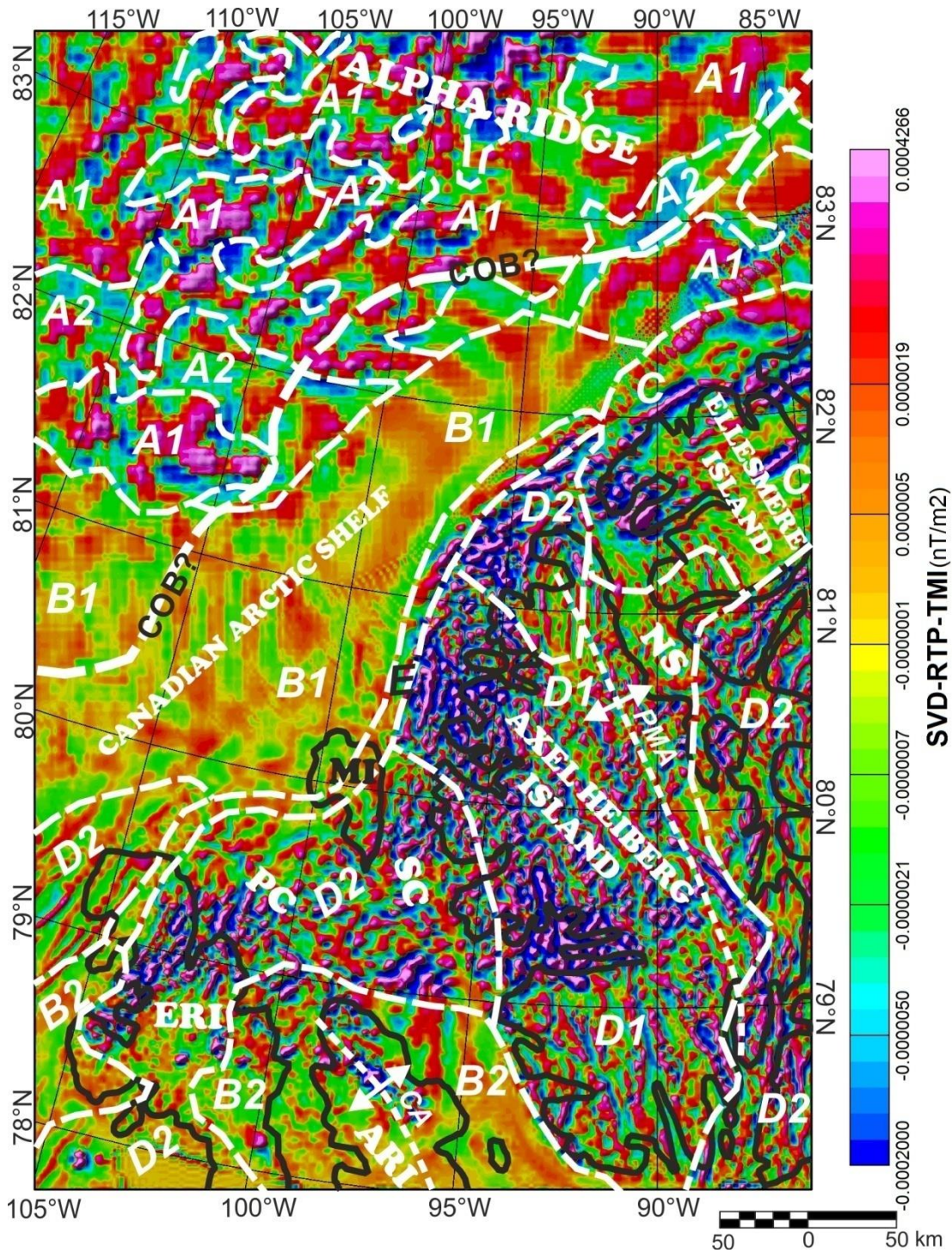


Figure 7. Second vertical derivative of Reduced to Pole total magnetic intensity (SVD-RTP-TMI) anomaly map of the study area. The edges of high amplitude, short wavelength magnetic anomalies associated with the underlying magmatic rock bodies and other tectonic features are greatly enhanced, delineated and mapped on the figure.

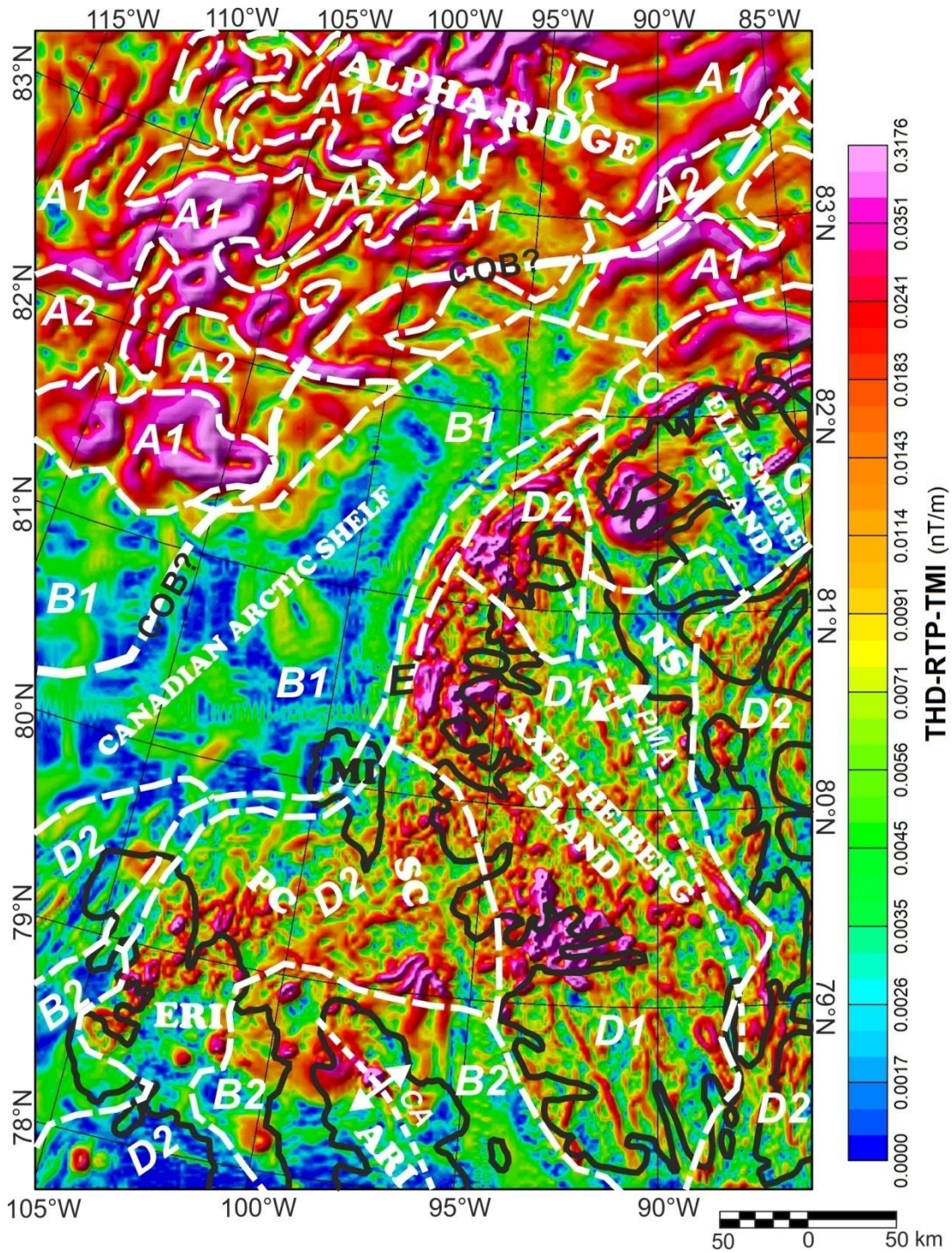


Figure 8. Total horizontal derivative of Reduced to Pole total magnetic intensity (THD-RTP-TMI) anomaly map of the study area. The edges of high amplitude, short wavelength magnetic anomalies associated with the underlying magmatic rock bodies and other tectonic features are greatly enhanced, delineated and mapped on the figure.

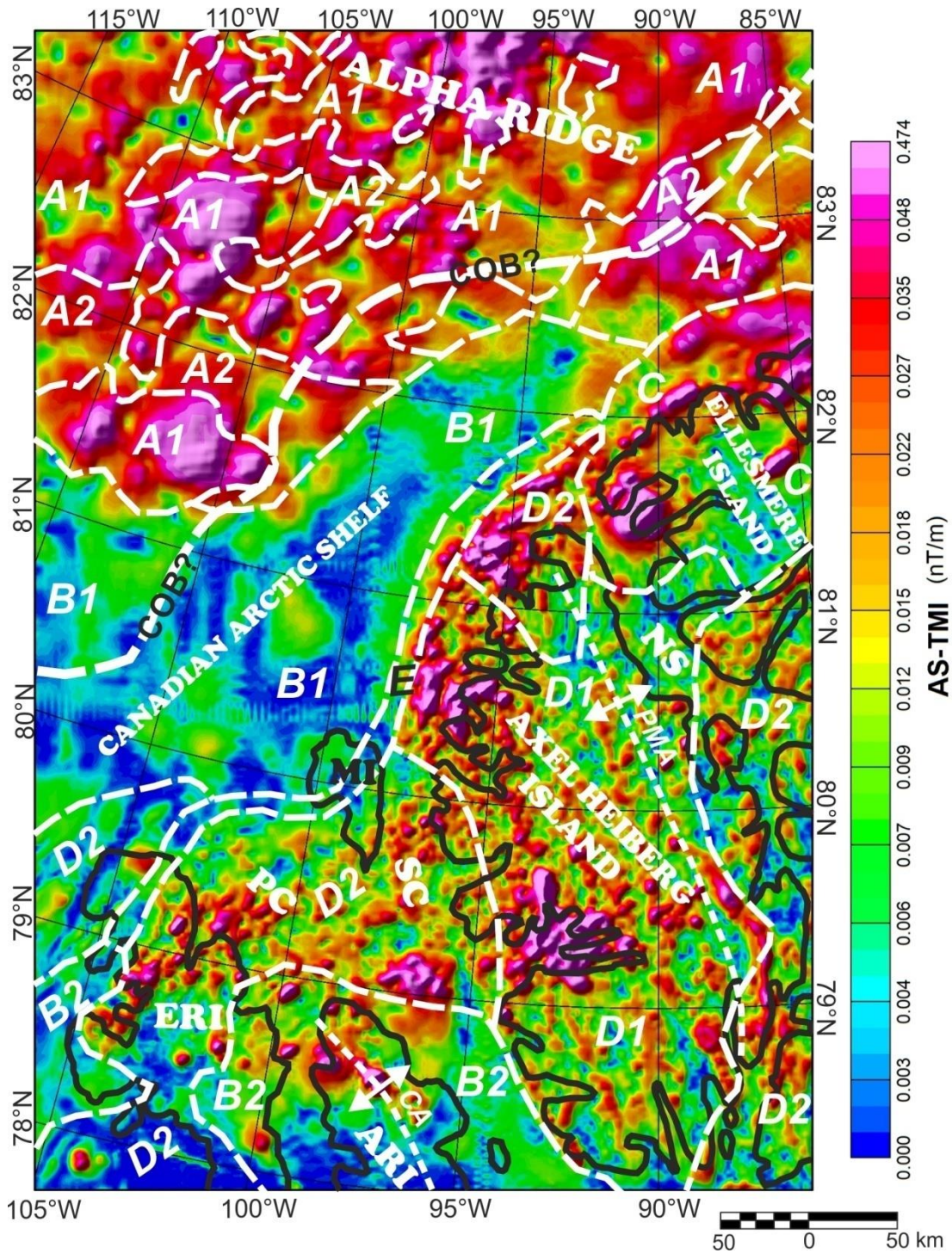


Figure 9. Analytic signal total magnetic intensity (AS-TMI) anomaly map of the study area. The edges of high amplitude, short wavelength magnetic anomalies associated with the underlying magmatic rock bodies and other tectonic features are greatly enhanced, delineated and mapped on the figure.

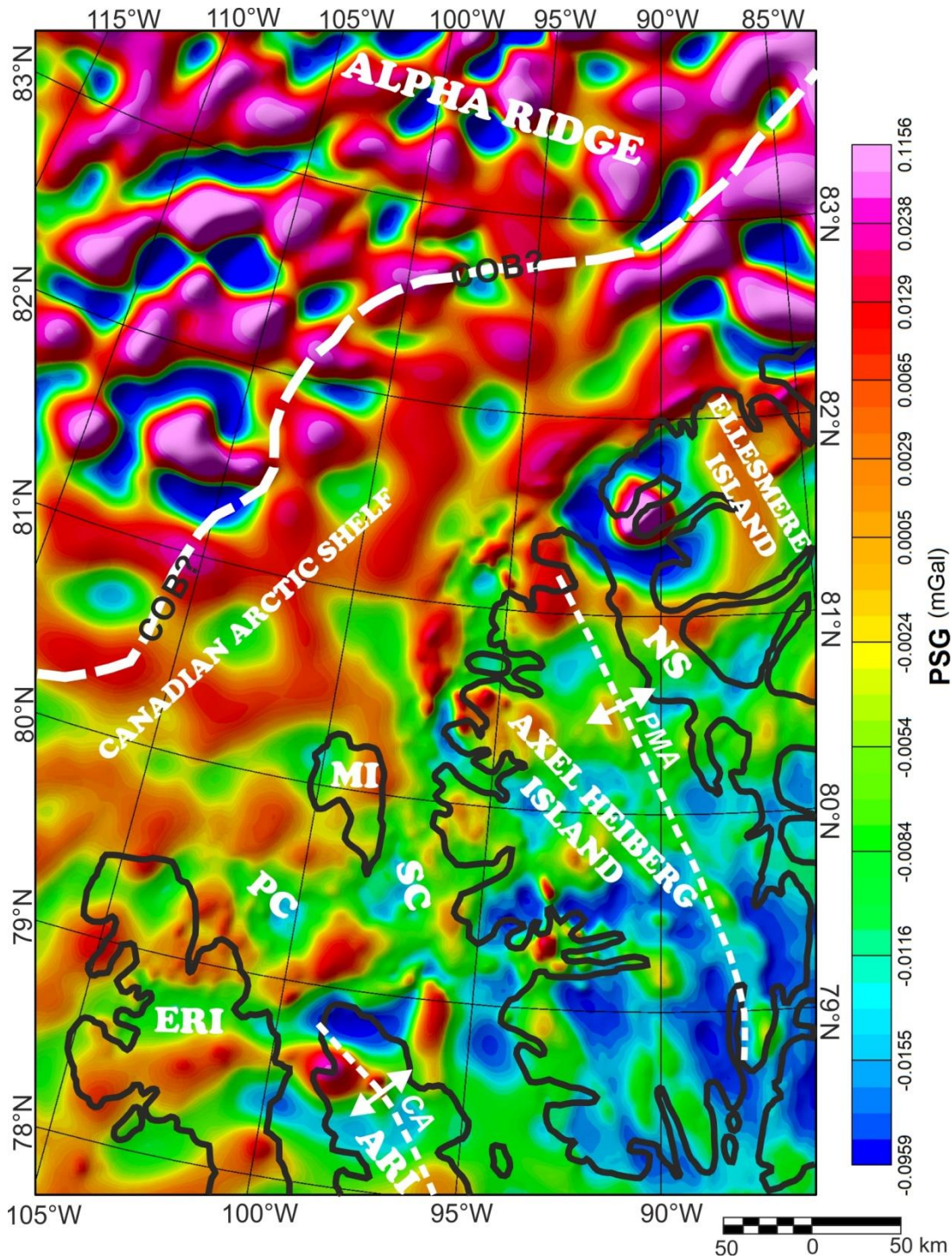


Figure 10. Pseudogravity (PSG) anomaly map of the study area. It shows the general variations in magnetisation of crustal rocks across the area.

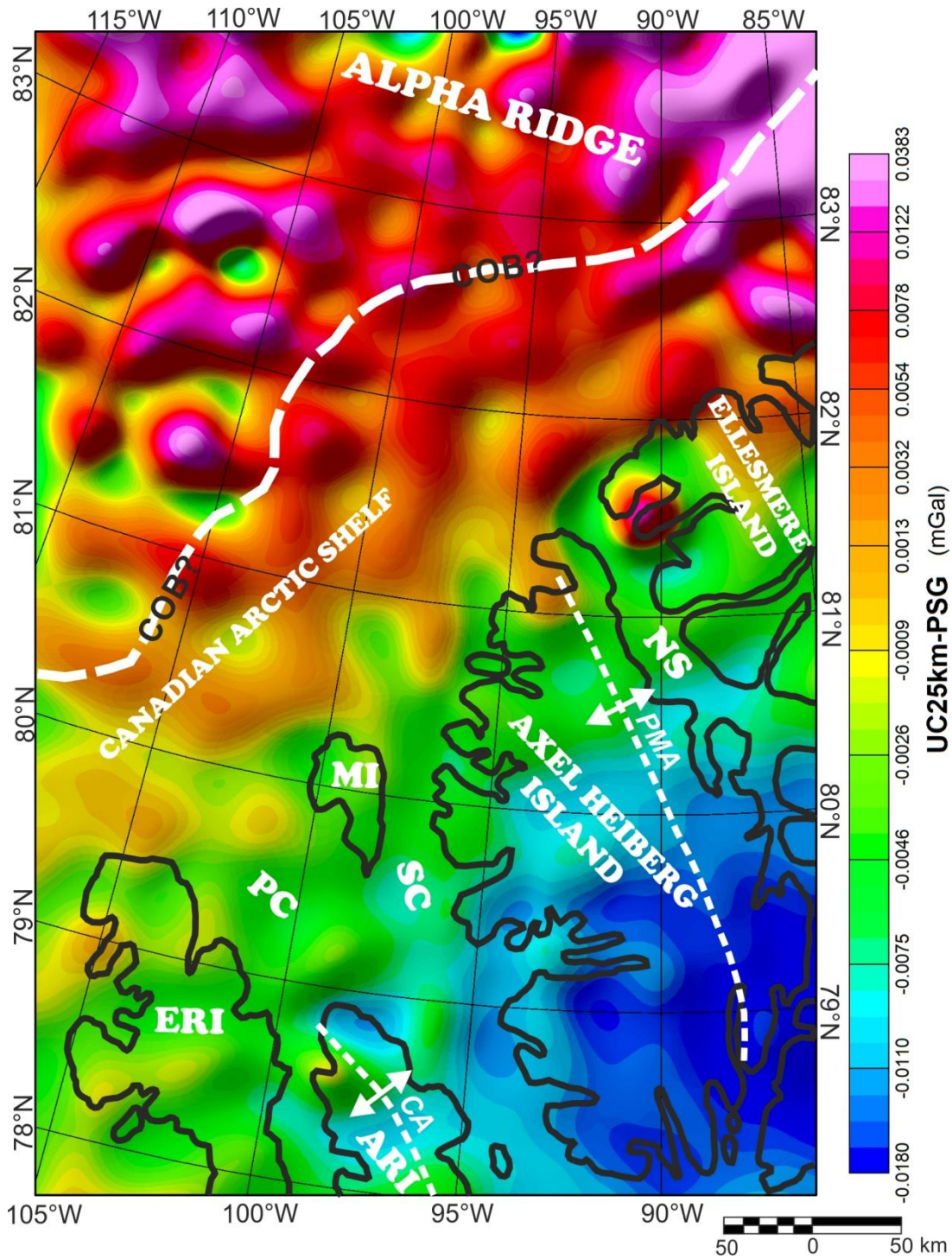


Figure 11. Upward continued 25 km pseudogravity (UC25km-PSG) anomaly map of the study area. It further highlights the variations in crustal rock magnetisation across the area. It reveals that the upper crustal rocks beneath the Alpha Ridge, Canadian Arctic Shelf and Sverdrup Basin regions exhibit high magnetisation, medium magnetisation and low magnetisation, respectively.

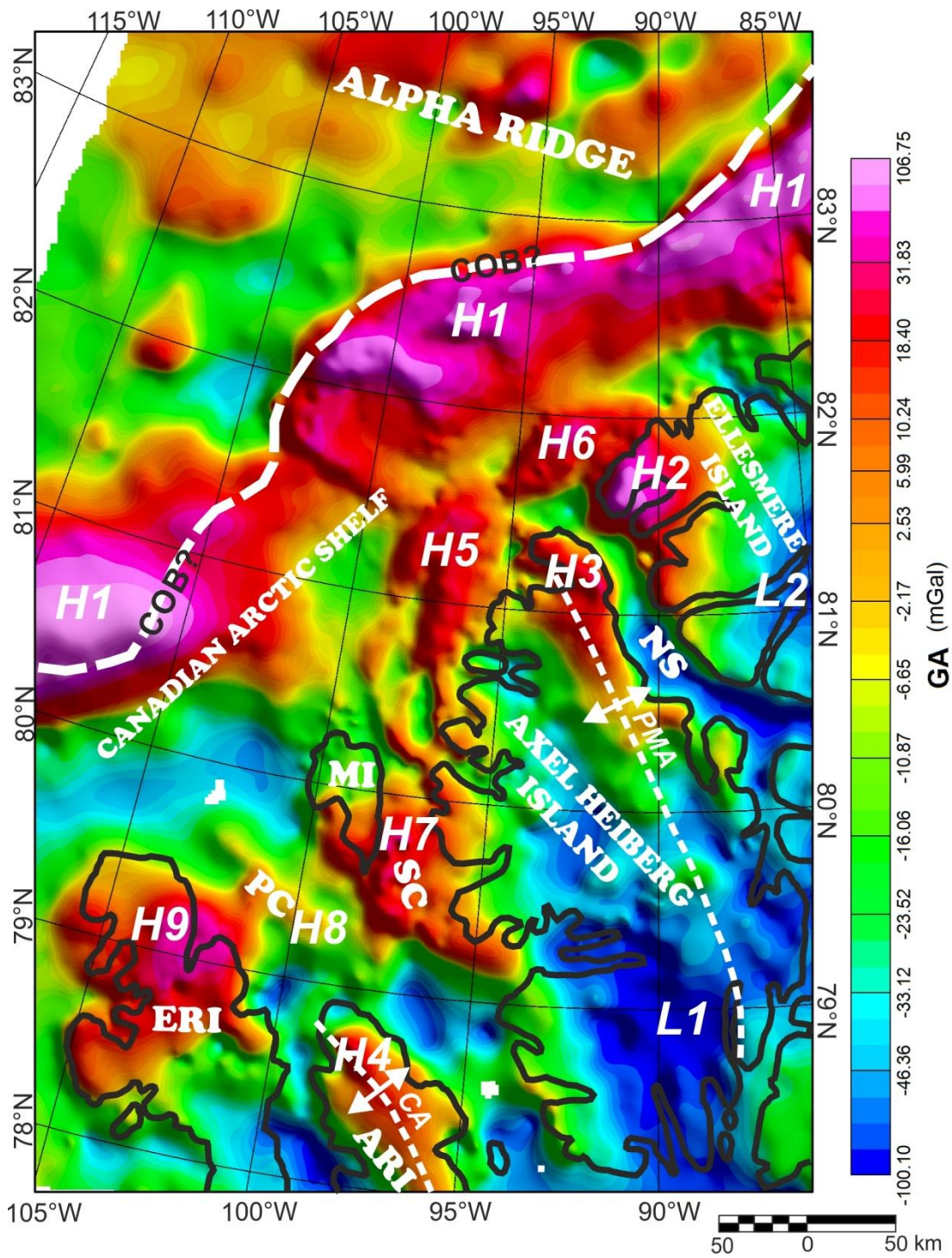


Figure 12. Gravity (Bouguer onshore, Free-Air offshore) anomaly map of the study area. Marked prominent gravity anomaly highs (H1 – H9) and lows (L1 – L2) are discussed in Section 5.3 of this paper.

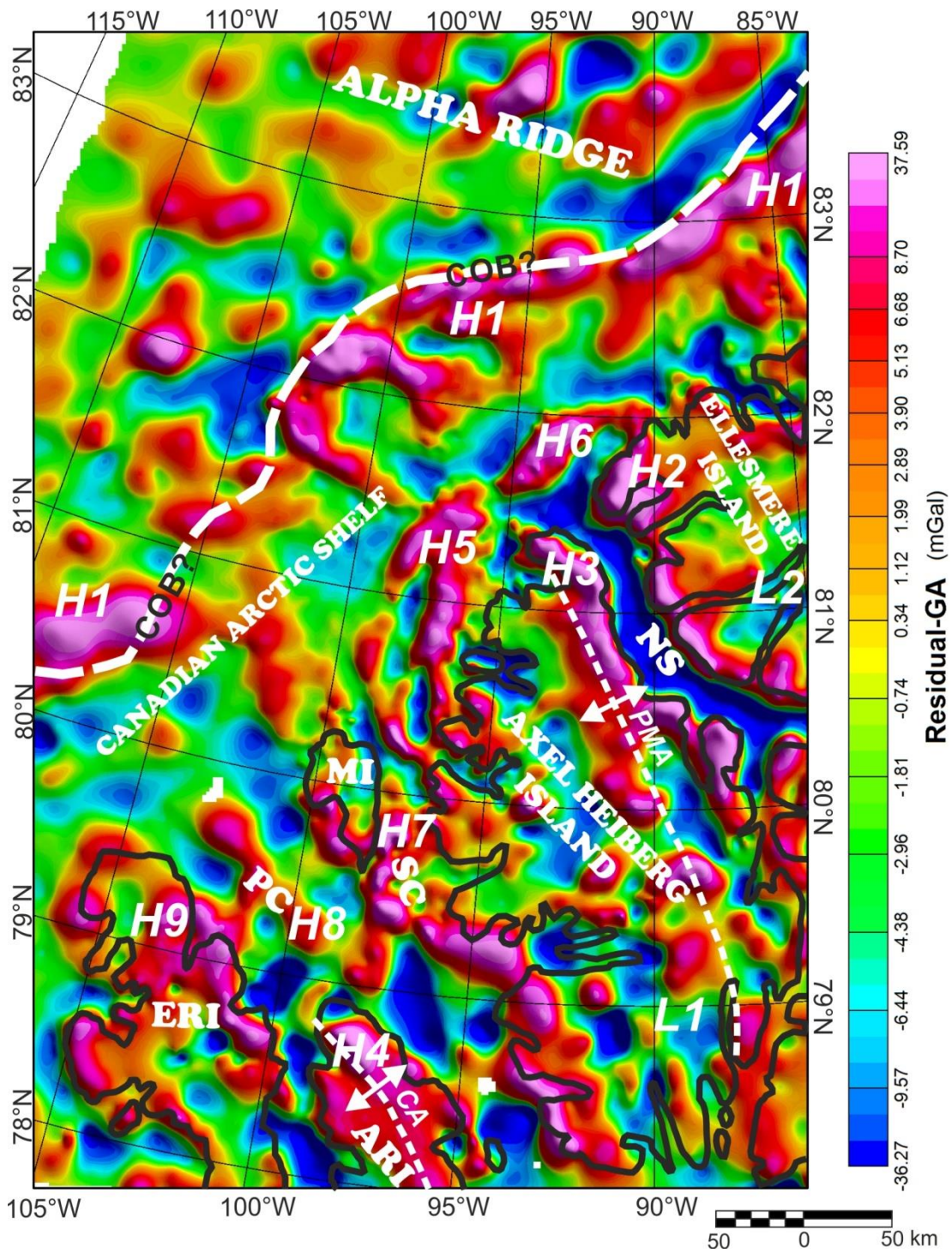


Figure 13. Residual gravity anomaly map of the study area. The underlying causative geological and/or tectonic features are greatly enhanced, delineated and mapped on the map.

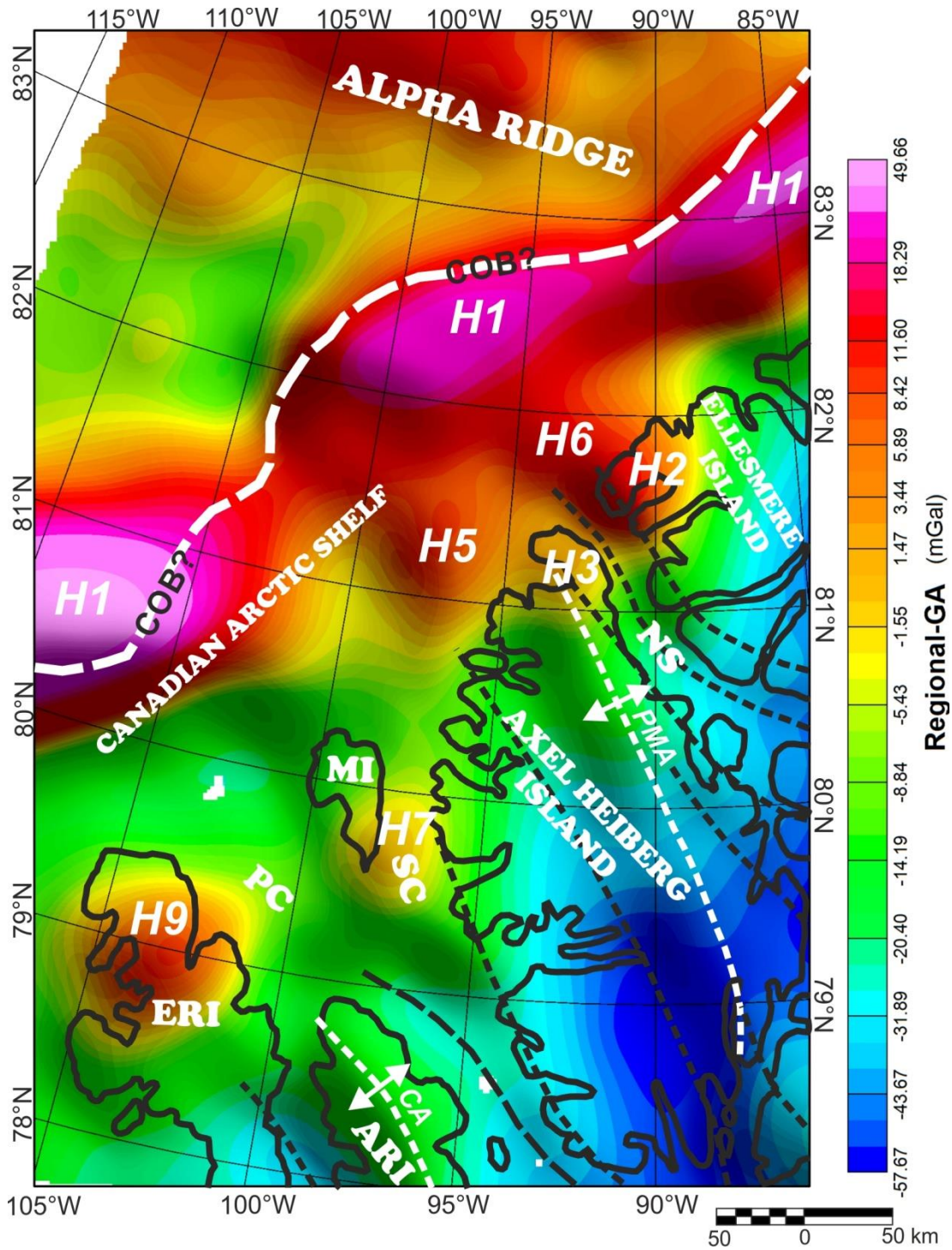


Figure 14. Regional gravity anomaly map of the study area. Dashed black lines are anticlinal and synclinal features, and are indications of “crustal folding” in the area. The underlying compressional tectonic structures (i.e. “crustal folding”) in the southern, southeastern and eastern regions of the study area are greatly enhanced on the map and two of the anticlinal structures coincide with the Princess Margaret Arch (PMA) and Cornwall Arch (CA).

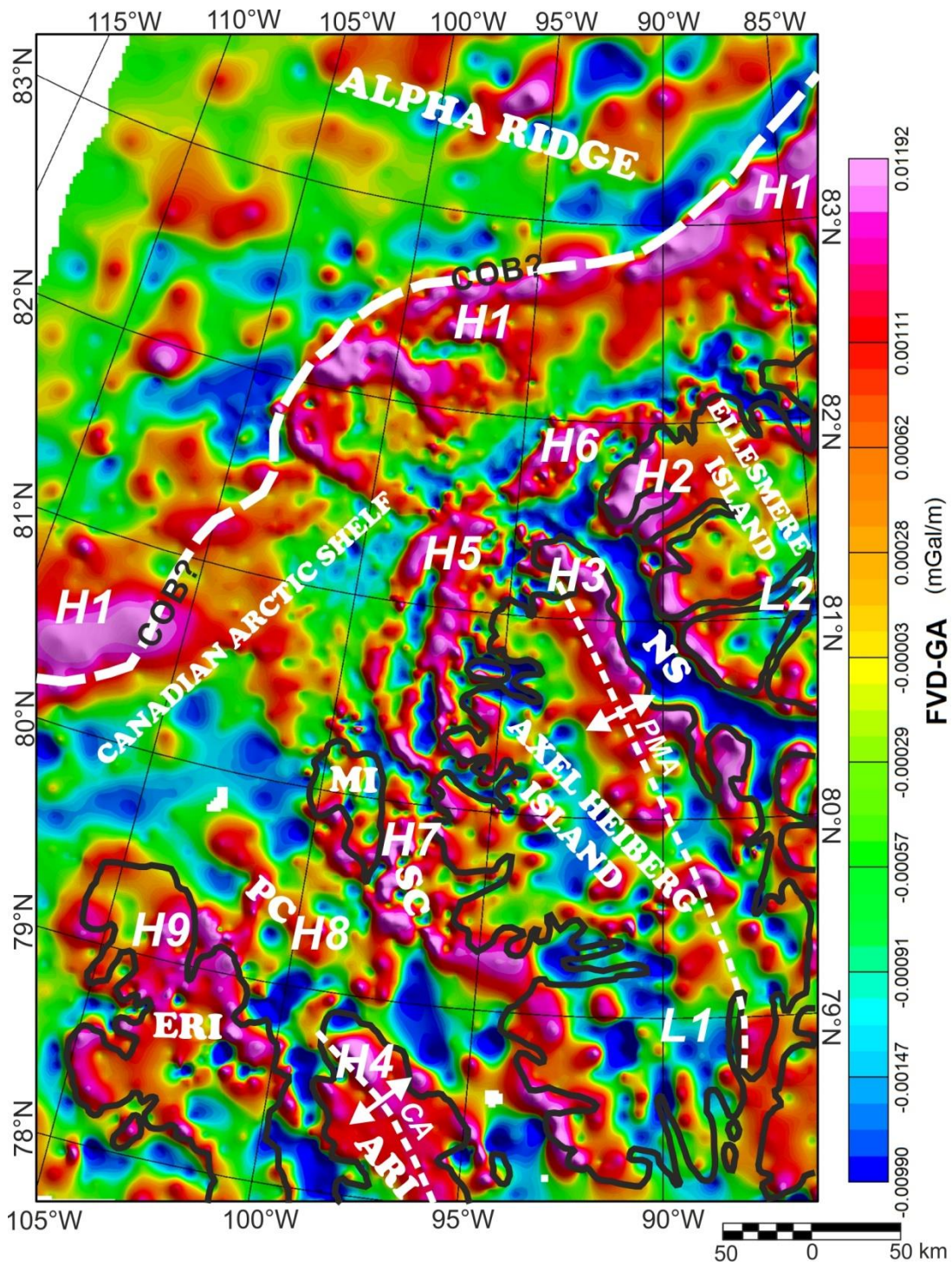


Figure 15. First vertical derivative (FVD) gravity anomaly map of the study area. It enhances and delineates the underlying shallow causative geological and/or tectonic features.

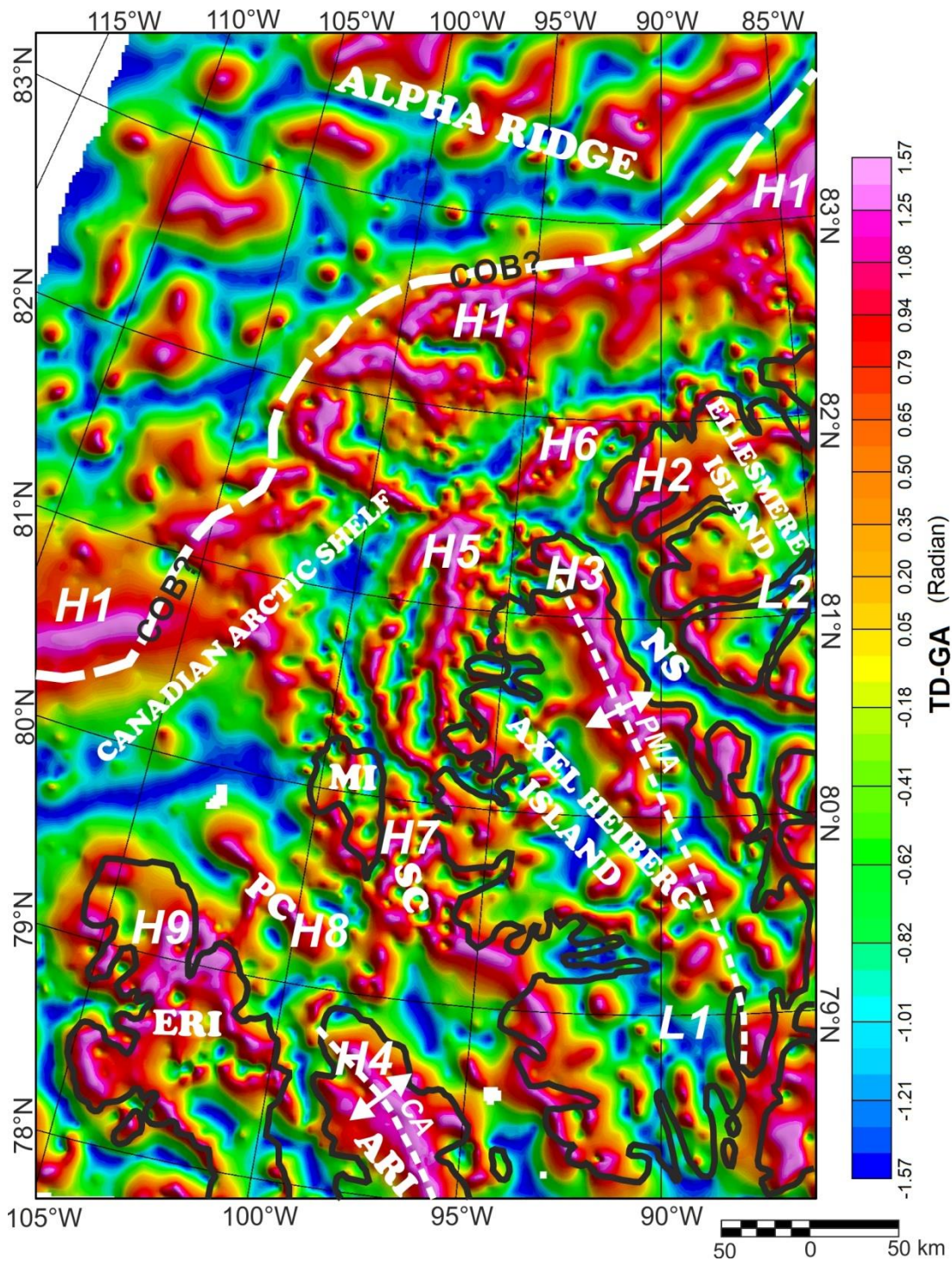


Figure 16. Tilt derivative (TD) gravity anomaly map of the study area. Although it is relatively similar to the FVD gravity map, it has higher spatial and structural resolution. Thus it greatly enhances, delineates and map both shallow and relatively deep causative geological and/or tectonic features across the area. The maxima on this map define the extent and edges of the causative features across the area.

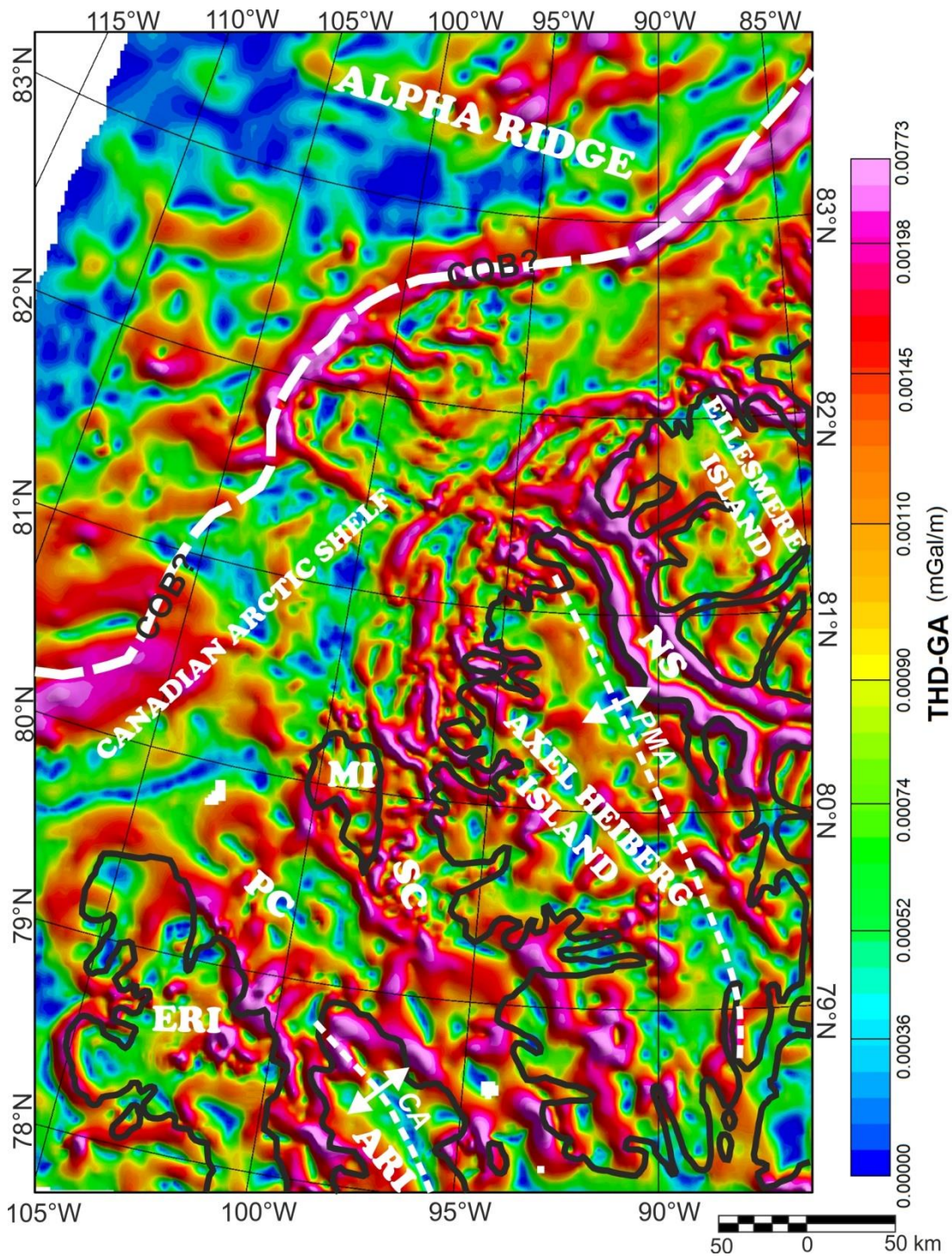


Figure 17. Total horizontal derivative (THD) gravity anomaly map of the study area. The maxima (ridges) on this map delineate and image edges of the causative (both the large-scale and subtle) geological and tectonic features associated with crustal basement fabrics/grains and other shallow tectonic (structural) fabric. It can be likened to a structural map of the area. The regional, well-defined maxima on this map (dashed white line) around the offshore Canadian Arctic Shelf – Alpha Ridge regions highlights and coincides with the ‘continent-ocean boundary’ (COB?) previously postulated by [Oakey and Stephenson \(2008\)](#).

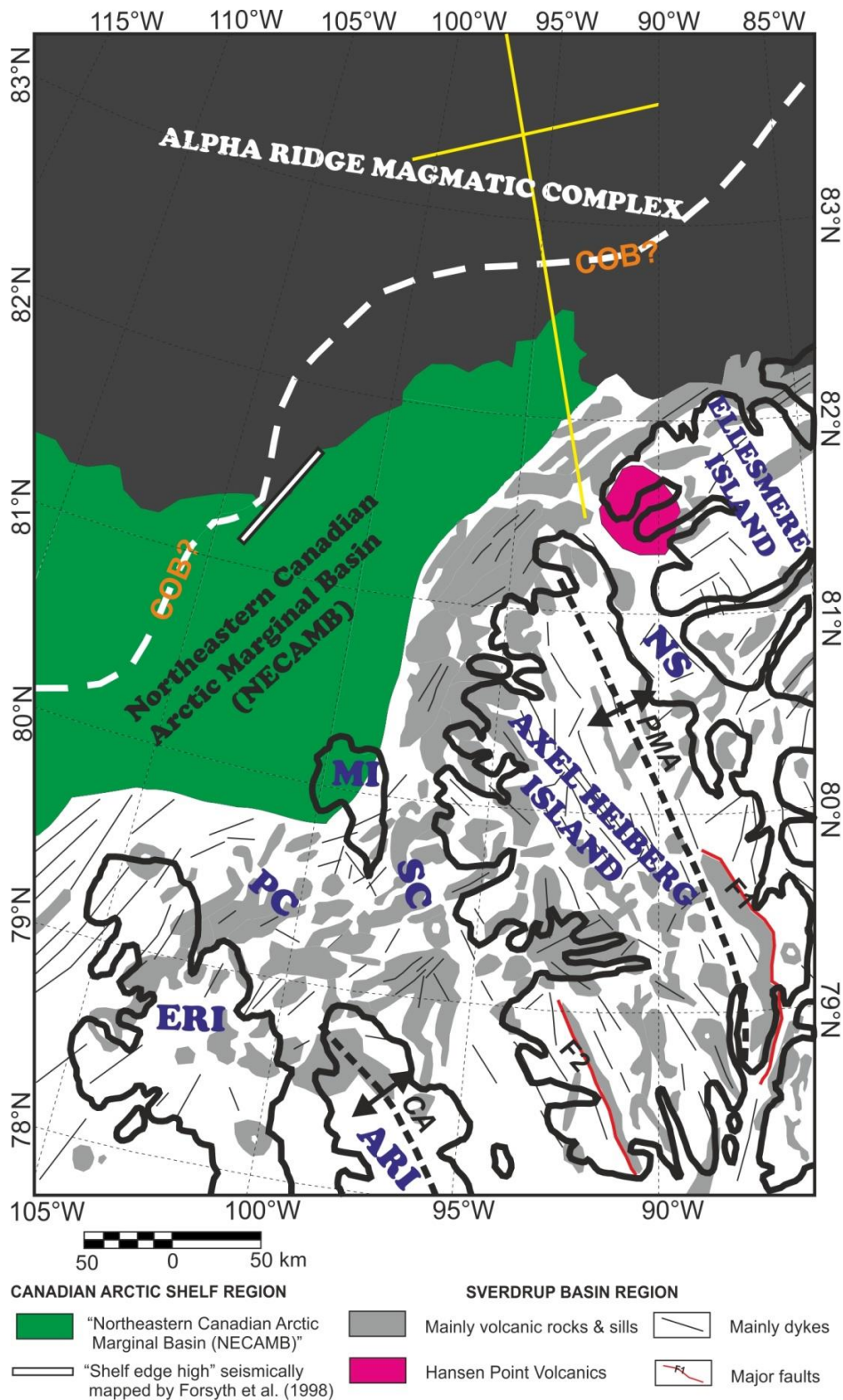


Figure 18. Magmatic intrusion distribution map derived from the edge enhanced (derivative) magnetic anomaly maps of the study area. Major sedimentary sub-basin well delineated and mapped beneath the Canadian Arctic Shelf region (and named the "Northeastern Canadian Arctic Marginal Basin (NECAMB)") is also shown. Two prominent geological faults mapped (F1 and F2; red lines) are the Stolz Thrust Fault (F1) and another fault (F2) trending NW-SE named here the 'South Strand Bay Fault'; both geological faults are represented on the magnetic maps by abrupt truncations of linear anomalies and coincident high gradients. Both faults are also recognised on all the gravity anomaly maps, with the exception of the regional gravity map. Yellow lines mark the ARTA 2008 seismic refraction profiles (Funck et al., 2011).